Electronic Supplementary Material (ESI) for Physical Chemistry Chemical Physics.

Electronic Supporting Information

Contrasting Luminescence in Heparin and DNA-templated Co-assemblies of Dimeric Cyanostilbenes: Efficient Energy Transfer in Heparin-based Co-assemblies

Dhananjoy Maity‡, Shubhra K. Bhaumik‡ and Supratim Banerjee*

Corresponding Author

*Supratim Banerjee- The Department of Chemical Sciences, Indian Institute of Science Education and Research Kolkata, Mohanpur 741246, Nadia, India; Email: supratim.banerjee@iiserkol.ac.in; ORCID- orcid.org/0000-0001-8558-4444

‡These authors contributed equally.

Table of Contents — Page No.

Experimental Procedures

1. Synthetic Procedure and Characterization Data:

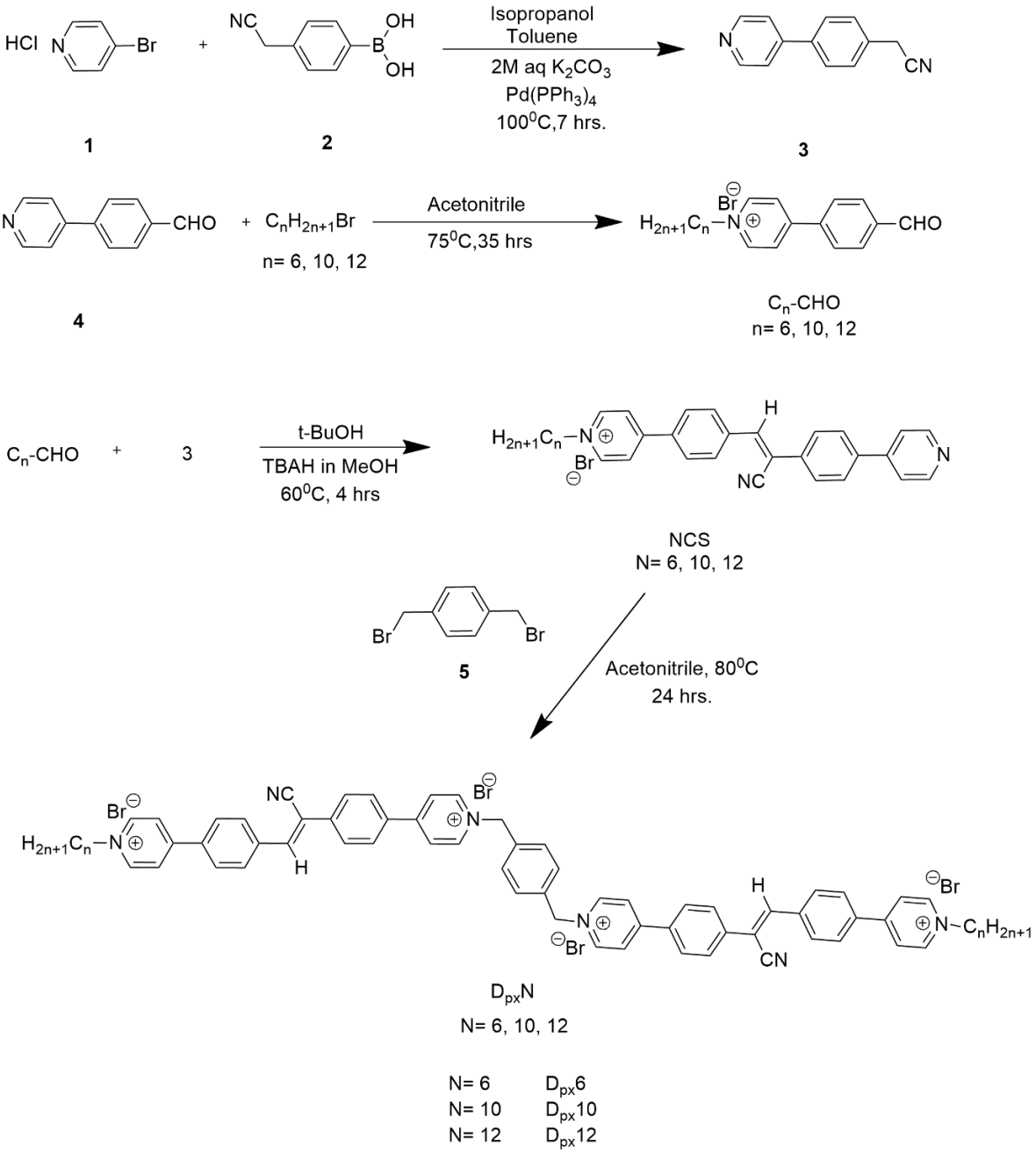

Scheme S1. Synthetic route of **D_{px}N (N=6, 10, 12)**

Synthesis of 3

4-(4-cyanomethyl)phenylboronic (**2**) acid (500 mg, 3.11 mmol) and 4-bromopyridine hydrochloride (**1**) (500 mg, 2.57 mmol) was added in a round bottom flask followed by addition of isopropanol (4.5 mL), toluene (4.5 mL) and 2M K_2CO_3 (6 mL). The solution was stirred for 30 minutes at 100 °C under N_2 atmosphere. Then $Pd(PPh_3)_4$ (89 mg, 0.06 mmol) was added and the mixture was finally refluxed for 7 hrs under N_2 atmosphere. The reaction mixture was

allowed to cool to room temperature and then poured into 50 mL water. Then, the crude was extracted by ethyl acetate and dried over anhydrous Na_2SO_4. Then the desired product was purified from the crude by using column chromatography (solid phase: silica gel 100-200 mesh, eluent: 50% ethyl acetate/hexane). Solvent was evaporated and finally dried under vacuum. Yield ~ 98%.

General procedure for synthesis of C_n-CHO (n=6, 10, 12)

4-(4-pyridinyl) benzaldehyde (**4**) (200 mg, 1.09 mmol) and alkyl bromide (21.9 mmol) were taken into a 10 mL round bottom flask and then 1.5 mL acetonitrile was added into it. The reaction mixture was stirred at 80 °C for 35 hrs and then allowed to cool at room temperature. A light-yellow colour semi solid crude obtained after removal of excess amount of acetonitrile was by rotavapor. Further, the crude was purified by using column chromatography (solid phase: neutral alumina, eluent: 5% MeOH in DCM). Yield ~ 80-90%.

^{1}H NMR for C_6-CHO (500 MHz, $CDCl_3$): δ (ppm) = 10.01 (s, 1H), 9.59 (d, *J*=8.0 Hz, 2H), 8.38 (d, *J*=8.0 Hz, 2H), 7.95-7.96 (m, 4H), 4.859 (t, *J*=9.0 Hz, 2H), 1.987 (quintet, *J*=9.0 Hz, 2H), 1.18 (m, *J*=7.0 Hz, 2H), 0.703 (t, *J*=8.5 Hz, 3H); **^{13}C NMR for C_6-CHO (125 MHz, $CDCl_3$)**: δ(ppm) = 191.21, 154.20, 145.35, 138.68, 138.06, 130.57, 128.66, 125.80, 61.23, 31.57, 30.89, 25.52, 22.12, 13.71; **MS (ESI):** m/z calculated for $C_{18}H_{22}NO^+$: 268.1696; Found: 268.1681.

^{1}H NMR for C_{10}-CHO ($CDCl_3$, 500 MHz): δ (ppm) =9.93 (s, 1H), 9.48 (d, *J*=6.5 Hz, 2H), 8.33 (d, *J*=6.5 Hz, 2H), 7.89-7.90 (m, 4H), 4.79 (t, *J*=7.5 Hz, 2H), 1.91 (quintet, *J*=7.5 Hz, 2H), 1.22 (quintet, *J*=8.0 Hz, 2H), 1.13 (quintet, *J*=6.5 Hz, 2H), 0.997 (m, 10H), 0.625 (t, *J*=7.0 Hz, 3H); **^{13}C NMR for C_{10}-CHO (125 MHz, $CDCl_3$)**: δ(ppm) = 191.05, 154.38, 145.25, 138.56, 137.97, 130.45, 128.54, 125.68, 61.13, 31.55, 31.43, 29.09, 29.01, 28.84, 28.75, 25.81, 22.25, 13.74; **MS (ESI):** m/z calculated for $C_{22}H_{30}NO^+$: 324.2322; Found: 324.2315.

^{1}H NMR for C_{12}-CHO ($CDCl_3$, 400 MHz): δ (ppm) = 10.02 (s, 1H), 9.57 (d, *J*=5.0 Hz, 2H), 8.4 (d, *J*=5.0 Hz, 2H), 8.97-8.98 (m, 4H), 4.87 (t, 2H), 2.0 (quintet, 2H), 1.3-1.11 (m, 18H), 0.74 (t, *J*=5.0 Hz, 3H); **^{13}C NMR for C_{12}-CHO (125 MHz, $CDCl_3$)**: δ(ppm) = 191.18, 154.37, 145.23, 138.59, 137.98, 130.49, 128.63, 125.75, 61.24, 31.57, 29.28, 29.23, 29.10, 29.00, 28.83, 25.89, 22.35, 13.82; **MS (ESI):** m/z calculated for $C_{24}H_{34}NO^+$: 352.2635; Found: 352.2635.

General procedure for synthesis of NCS (N=6, 10, 12)

(4-Pyridin-4-yl-phenyl)-acetonitrile (**3**) (113 mg, 0.58 mmol) and C_n-CHO (0.58 mmol) were added in a round bottom flask followed by addition of 3 mL *tert*-butanol and this mixture was stirred for 30 min at 60 °C. Tetrabutylamonium hydroxide in methanol solution (1 M) (0.058 mL, 0.1 eq) was taken in a vial and then it was diluted four time in by methanol. This solution was added dropwise into the round bottom flask containing reaction mixture until light yellow coloration was observed. Then this reaction mixture was stirred for 3 hrs. A yellow crude was obtained after washing with hot *tert*-butanol. The product was further purified by using column chromatography (solid phase: neutral alumina, eluent: 5% MeOH in DCM). Yield ~70-80%.

^{1}H NMR for 6CS (400 MHz, DMSO-D$_6$): δ(ppm) = 9.19 (d, *J*=8.0 Hz, 2H), 8.68 (d, *J*=8.0 Hz, 2H), 8.62 (d, *J*=8.0 Hz, 2H), 8.31 (d, *J*=8.0 Hz, 2H), 8.29 (s, 1H), 8.20 (d, *J*=8.0 Hz, 2H), 8.01 (d, *J*=8.0 Hz, 2H), 7.97 (d, *J*=8.0 Hz, 2H), 7.80 (d, *J*=4.0 Hz, 2H), 4.61 (t, *J*=8.0 Hz, 2H), 1.95 (quintet, *J*=6.0 Hz, 2H), 1.31 (m, 6H), 0.87 (t, *J*=6.0 Hz, 3H)); **^{13}C NMR for 6CS (100 MHz, DMSO-D$_6$)**: δ(ppm) = 153.35, 150.34, 145.65, 144.87, 141.84, 138.10, 136.91, 134.97, 134.13, 130.16, 128.69, 127.61, 126.74, 124.59, 121.11, 117.46, 111.66, 59.98, 31.28, 30.57, 25.08, 21.84, 13.81: **MS (ESI):** m/z calculated for $C_{31}H_{30}N_3^+$: 444.2434; Found: 444.2434.

^{1}H NMR for 10CS (500 MHz, 17%CDCl$_3$ in DMSO-D$_6$): δ(ppm) = 9.18 (d, *J*=7.0 Hz, 2H), 8.67 (d, *J*=7.0 Hz, 2H), 8.60 (d, *J*=7.0 Hz, 2H), 8.27 (t, *J*=7.0 Hz, 2H), 8.20 (d, *J*= 9.0 Hz, 2H), 7.97 (t, *J*=9.0 Hz, 4H), 7.77 (d, *J*=6.0 Hz, 2H), 4.615 (t, *J*=7.0 Hz, 2H), 1.956 (quintet, *J*=7.0 Hz, 2H), 1.319-1.220 (m, 14H), 0.85 (t, *J*=6.5 Hz, 3H); **^{13}C NMR for 10CS (125 MHz, 17%CDCl$_3$ in DMSO-D$_6$)**: δ(ppm) = 153.48, 150.02, 145.87, 144.80, 141.60, 138.07, 136.87, 134.85, 134.13, 130.10, 128.54, 127.49, 126.66, 124.56, 121.06, 117.27, 111.74, 59.98, 31.19, 30.68, 28.80, 28.73, 28.56, 28.35, 25.39,21.99, 20.87: **MS (ESI):** m/z calculated for $C_{35}H_{38}N_3^+$: 500.3060; Found: 500.3071.

^{1}H NMR for 12CS (400 MHz, DMSO-D$_6$): δ(ppm) = 9.17 (d, *J*=7.0 Hz, 2H), 8.68 (d, *J*=6.0 Hz, 2H), 8.61 (d, *J*=7.0 Hz, 2H), 8.32 (d, *J*=6.0 Hz, 2H), 8.31 (t, *J*=8.5 Hz, 2H), 8.02 (d, *J*=8.5 Hz, 2H), 7.97 (d, *J*=8.5 Hz, 2H), 7.81 (d, *J*=6.0 Hz, 2H), 4.597 (t, *J*=7.0 Hz, 2H), 1.95 (quintet, 2H), 1.30-1.23 (m, 18H), 0.84 (t, *J*=6.0 Hz, 2H); **^{13}C NMR for 12CS (125 MHz, 17%CDCl$_3$ in DMSO-D$_6$)**: δ(ppm) = 153.35, 150.32, 145.65,144.86, 141.83, 138.09, 136.90, 134.90, 134.96, 134.13, 130.15, 128.67, 127.59, 126.73, 124.58, 121.09, 117.44, 111.65, 59.98, 31.09,

30.61, 28.41, 28.33, 25.41, 21.98, 13.88: **MS (ESI):** m/z calculated for $C_{37}H_{42}N_3^+$: 528.3373; Found: 528.3370

General procedure for synthesis of $D_{px}N$ (N=6, 10, 12)

NCS (0.043 mmol) and p-xylene dibromide (**5**) (4.6 mg, 0.017 mmol) were taken into a round bottom flask and then 1 mL acetonitrile was added into it. The reaction mixture was stirred at 80 °C for 24 hrs and then allowed to cool to room temperature. A yellow-coloured precipitation was observed which was purified by washing with methanol/DCM (1:1) mixture. Yield~ 80-90%.

^{1}H NMR for D_{px}6 (400 MHz, DMSO-D_6): δ(ppm) = 9.32 (d, *J*=7.0 Hz, 4H), 9.19 (d, *J*=7.0 Hz, 4H), 8.66 (d, *J*=7.0 Hz, 4H), 8.63(d, *J*=7.0 Hz, 4H), 8.54 (s, 2H), 8.33 (d, *J*=8.0 Hz, 4H), 8.29 (d, *J*=8.0 Hz, 4H), 8.23 (d, *J*=8.0 Hz, 4H), 8.09 (d, *J*=8.0 Hz, 4H), 7.71 (s, 4H), 5.92 (s, 4H), 4.62 (t, *J*=7.0 Hz, 4H), 1.95 (quintet, *J*=6.8 Hz, 14H), 1.32 (m, 12H), 0.884 (t, *J*=7.0 Hz, 6H); **^{13}C NMR for D_{px}6 (125 MHz, DMSO-D_6)**: δ(ppm) = 153.89, 153.32, 144.97, 144.91, 143.35, 136.87, 136.69, 135.50, 135.35, 134.18, 130.33, 129.53, 129.12, 128.75, 127.06, 125.03, 124.68, 117.68, 111.22, 61.90, 60.03, 30.58, 30.56, 25.07, 21.83, 13.08; **MS (ESI):** m/z calculated for $C_{70}H_{68}N_6^{4+}$: 248.1371; Found: 248.1364.

^{1}H NMR for D_{px}10 (400 MHz, DMSO-D_6): δ(ppm) = 9.31 (d, *J*=8.0 Hz, 4H), 9.185 (d, *J*=8.0 Hz, 4H), 8.65 (d, *J*=8.0 Hz, 4H), 8.62 (d, *J*=8.0 Hz, 4H), 8.44 (s, 4H), 8.32 (d, *J*=8.0 Hz, 4H), 8.28 (d, *J*=8.0 Hz, 4H), 8.23 (d, *J*=8.0 Hz, 4H), 8.08 (d, *J*=8.0 Hz, 4H), 7.70 (s, 4H), 5.91 (s, 4H), 4.61 (t, *J*=8.0 Hz, 4H), 1.96 (quintet, *J*=4.0-8.0 Hz, 4H), 1.31 (s, 28H), 0.85 (t, *J*=8.0 Hz, 6H); **^{13}C NMR for D_{px}10 (125 MHz, DMSO-D_6)**: δ(ppm) = 153.91, 153.34, 144.99,144.93, 143.37, 136.89, 136.71,135.51, 135.36, 134.20, 130.35, 129.55, 129.14, 128.76, 127.09, 125.05, 124.69, 117.30, 111.25, 61.97, 60.09, 31.26, 30.64, 28.85, 28.78, 28.63, 28.39, 25.43, 22.07, 13.94; **MS (ESI):** m/z calculated for $C_{78}H_{84}N_6^{4+}$: 276.1684 ; Found: 276.1694.

^{1}H NMR for D_{px}12 (400 MHz, DMSO-D_6): δ(ppm) = 9.30 (d, *J*=8.0 Hz, 4H), 9.18 (d, *J*=8.0 Hz, 4H), 8.65(d, *J*=8.0 Hz, 4H), 8.62 (d, *J*=8.0 Hz, 4H), 8.44 (s, 2H), 8.32 (d, *J*=8.0 Hz, 4H), 8.28 (d, *J*=8.0 Hz, 4H), 8.23 (d, *J*=8.0 Hz, 4H), 8.08 (d, *J*=8.0 Hz, 4H), 7.69 (s, 4H), 5.90 (s, 4H), 4.61 (t, *J*=8.0 Hz, 4H), 1.95 (quintet, *J*=6.0-8.0 Hz, 4H), 1.31-1.23 (m, 4H), 0.85 (d, *J*=6.0 Hz, 6H); **^{13}C NMR for D_{px}12 (125 MHz, DMSO-D_6)**: δ(ppm) =154.15, 153.54, 145.09, 145.03, 143.49, 137.01, 136.83, 135.56, 135.53, 134.35, 130.52, 129.75, 129.27, 128.88, 127.26, 125.20, 124.85, 117.45, 111.46, 62.22, 60.32, 31.40, 30.75, 29.11, 29.01, 28.89, 28.81,

28.51, 25.54, 22.20, 14.08; **MS (ESI):** m/z calculated for $C_{82}H_{92}N_6^{4+}$: 290.1840 ; Found: 290.1834.

2. Preparation of Solutions:

Preparation of solution of D_{px}Ns:

Initially, stock solutions of **D_{px}N**s (N = 6, 10, 12) were prepared by dissolving the solid powders in spectroscopic grade dimethyl sulfoxide (DMSO). The DMSO solutions were then diluted by 5 mM tris-HCl buffer made in Milli-Q water to get desired solutions having 1% DMSO as the final DMSO fraction. Solution of **D_{px}N**s in aqueous buffer were equilibrated for 30-40 min.

Preparation of heparin stock solution:

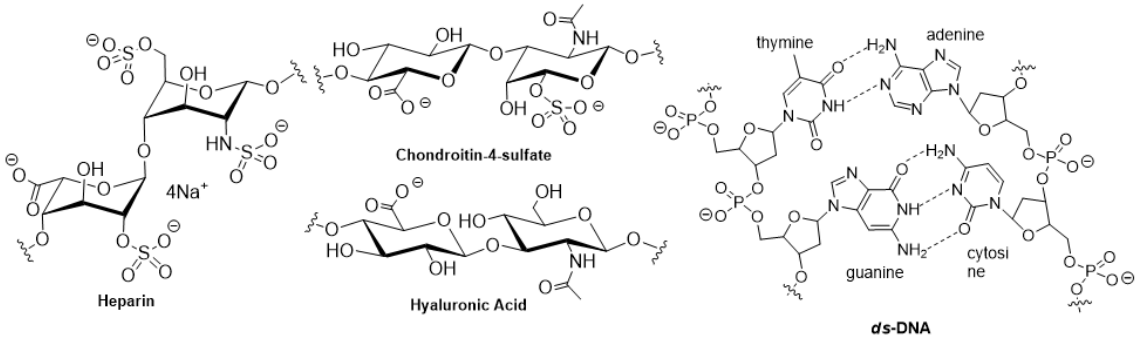

Chart S1 Common repeat units of heparin, chondroitin-4-sulfate (**ChS**), hyaluronic acid (**HA**), and double-stranded DNA (***ds*-DNA**)

The disaccharide unit shown in Fig. S1 is taken as the repeat unit of heparin for the molecular weight calculation. Though the supplied heparin contains only 30-40% materials with the active sequence of repeat units, the whole sample can still bind through the anionic polysaccharide unit irrespective of whether the repeat units are in active sequence or not. The molecular weight of the repeat unit is 665.40 g/mole. Heparin stock solutions were prepared in buffer and further diluted during titration.

Preparation of *ct*-DNA stock solution:

The *ct*-DNA stock was prepared by dissolving 1 mg of *ct*-DNA in 1 mL of 5 mM tris-HCl buffer (pH 7.40). The purity of *ct*-DNA was checked via monitoring the ratio of the absorbance at 260 and 280 nm, and the A_{260}/A_{280} ratio was found to be 1.87, indicating that *ct*-DNA was sufficiently free from protein contamination. The concentration of *ct*-DNA solution was spectrophotometrically calculated to be 2.03 mM using its known molar absorption coefficient e at 260 nm, which is 6600 M^{-1} cm^{-1}.

3. Titration Procedures:

At first, heparin solution was added to freshly prepared and equilibrated $\mathbf{D}_{px}\mathbf{N}$ solutions in aqueous buffer and further equilibrated for 10 min. Then different concentration of Nile Red dye were added to it and data were recorded in a spectrofluorometer after 5 min.

4. Energy Transfer Efficiency Calculation

Energy transfer (ET) efficiency is the percentage of the absorbed energy that is transferred to the acceptor and is expressed by the following equation

$$ET = (1 - I/I_0) \times 100\%$$

where, I and I_0 are the fluorescence intensities without and in presence of Nile Red (**NR**) in aqueous buffer.

5. Antenna Effect Calculation

The antenna effect (AE) value under certain concentrations of donor and acceptor is the ratio of the emission intensities at emission maximum of the acceptor in presence of the donor upon excitation of the donor and is expressed as follows-

$$AE = \frac{I_{\text{Em max. of A}}^{\text{D+A } (\lambda_{ex} = 365 \text{ nm})} - I_{\text{Em max. of A}}^{\text{D } (\lambda_{ex} = 365 \text{ nm})}}{I_{\text{Em max. of A}}^{\text{A } (\lambda_{ex} = \text{abs maxima of A})}}$$

where, $I_{\text{Em max. of A}}^{\text{D+A } (\lambda_{ex} = 365 \text{ nm})}$ = Emission intensity of acceptor in the presence of donor upon the excitation of donor

$I_{\text{Em max. of A}}^{\text{D } (\lambda_{ex} = 365 \text{ nm})}$ = Emission intensity of donor in the absence of acceptor upon the excitation of donor

$I_{\text{Em max. of A}}^{\text{A } (\lambda_{ex} = \text{abs maxima of A})}$ = Emission intensity of acceptor in the presence of donor upon the excitation of acceptor

Results and Discussion

1. Photo-physical Properties of D_{px}Ns

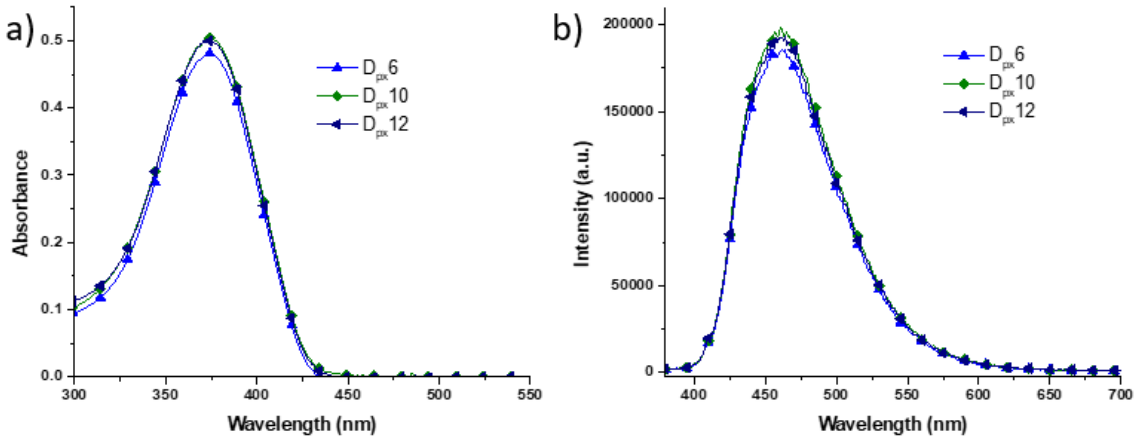

Fig. S1 (a) Absorption and (b) emission spectra of **D_{px}N** (N=6, 10, 12) at 5.0 µM in DMSO.

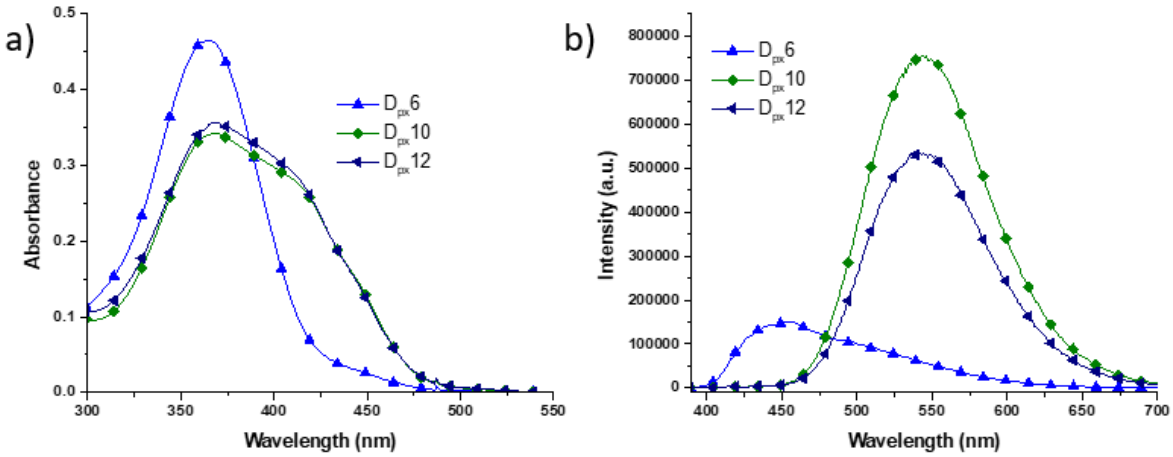

Fig. S2 (a) Absorption and (b) emission spectra of **D_{px}N** (N=6, 10, 12) at 5.0 µM in aqueous buffer (5 mM tris-HCl, 99:1 water-DMSO).

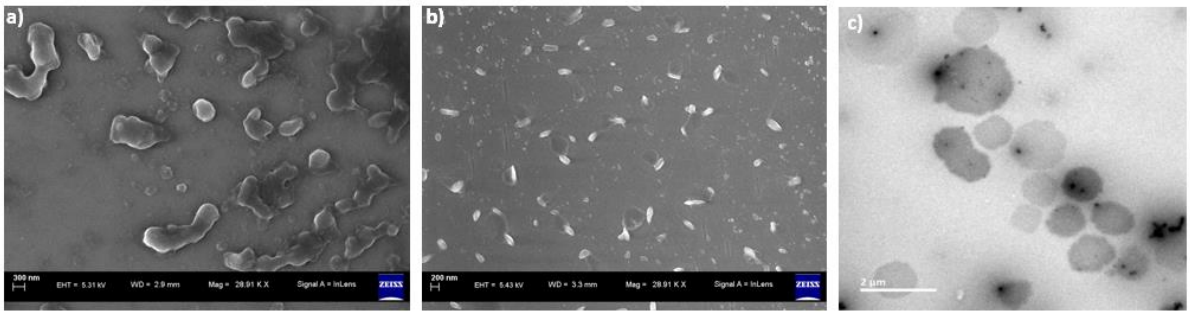

Fig. S3 FESEM images of (a) **D_{px}10** (5.0 µM) and (b) **D_{px}12** (5.0) µM dried from their aqueous solution. (c) TEM image of **D_{px}12** (5.0) µM dried from its aqueous solution.

Table S1 Fluorescence lifetime data of **D*px*Ns** in aqueous buffer (λ_{ex} = 340 nm).

D*px*N derivative	**λ_{em}**	**Lifetime (τ) parameters**	**Average lifetime (τ_{avg})**	**χ^2**
D*px*6 (5.0 µM)	453 nm	<0.2 ns (100%)	<0.2 ns	1.05
D*px*10 (5.0 µM)	545 nm	τ_1 = 1.80 ns (39%) τ_2 = 5.36 ns (61%)	3.97 ns	1.09
D*px*12 (5.0 µM)	545 nm	τ_1 = 1.88 ns (42%) τ_2 = 5.90 ns (58%)	4.21 ns	1.08

2. Heparin Binding Studies in Buffer

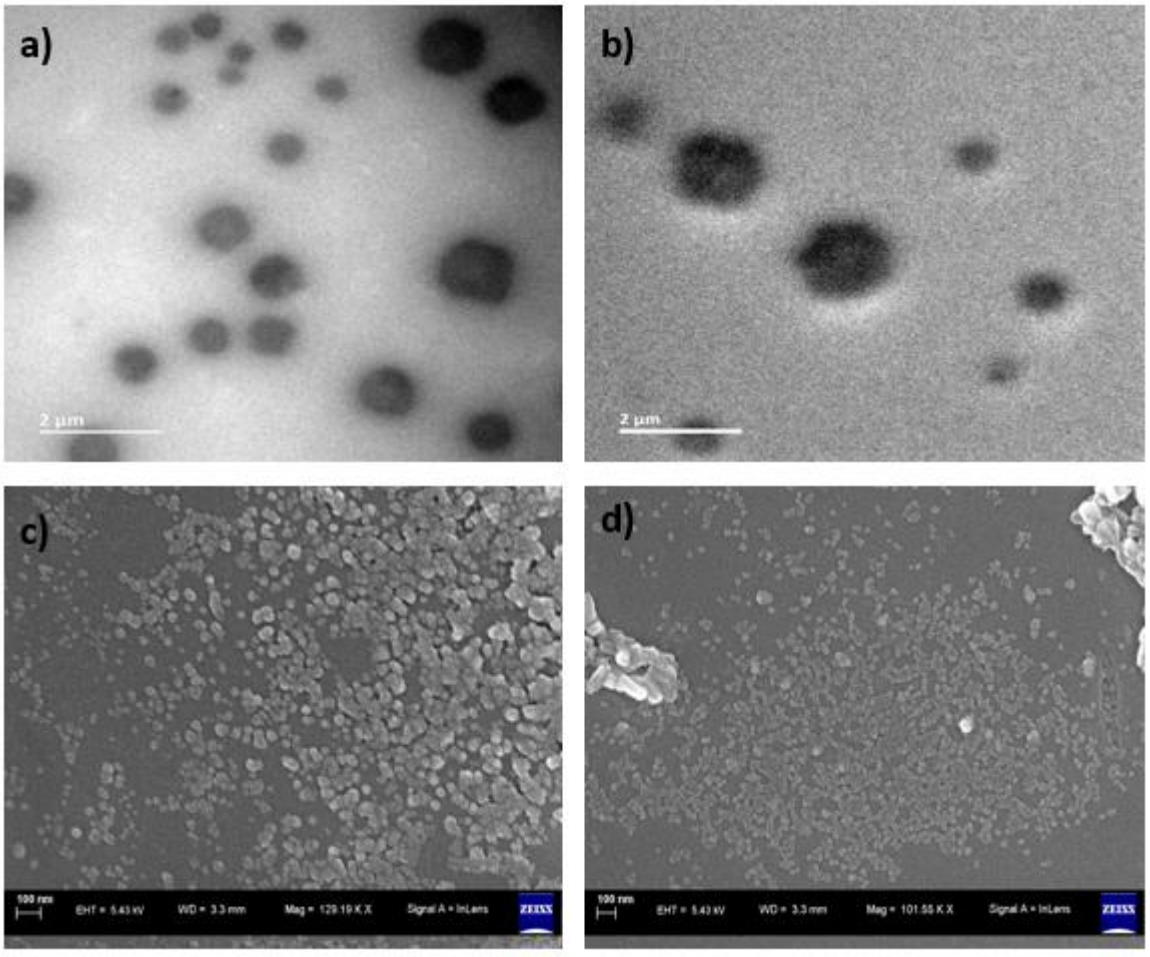

Fig S4. TEM images of (a) **D*px*10** (5.0 µM) and (b) **D*px*12** (5.0 µM), and FESEM images of (c) **D*px*10** (5.0 µM) and (d) **D*px*12** (5.0 µM) in the presence of heparin (10 µM) dried from its aqueous solution.

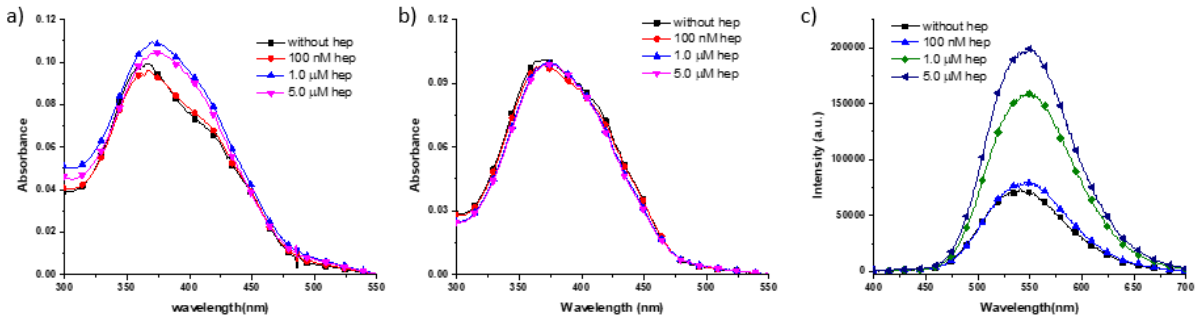

Fig. S5 Absorption spectral changes of (a) **D*px*10** (1.0 μM) and (b) **D*px*12** (1.0 μM), and (c) emission spectral changes of **D*px*12** (1.0 μM) upon addition of different amount of heparin in aqueous buffer (5 mM tris-HCl, 99:1 water-DMSO).

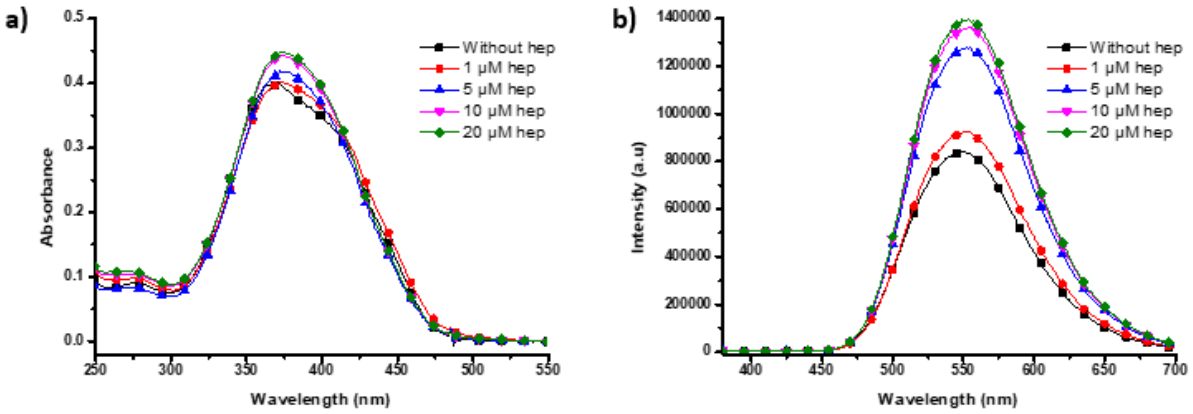

Fig. S6 (a) Absorption and (b) emission spectral changes **D*px*10** (5.0 μM) upon addition of different amount of heparin in aqueous buffer (5 mM tris-HCl, 99:1 water-DMSO).

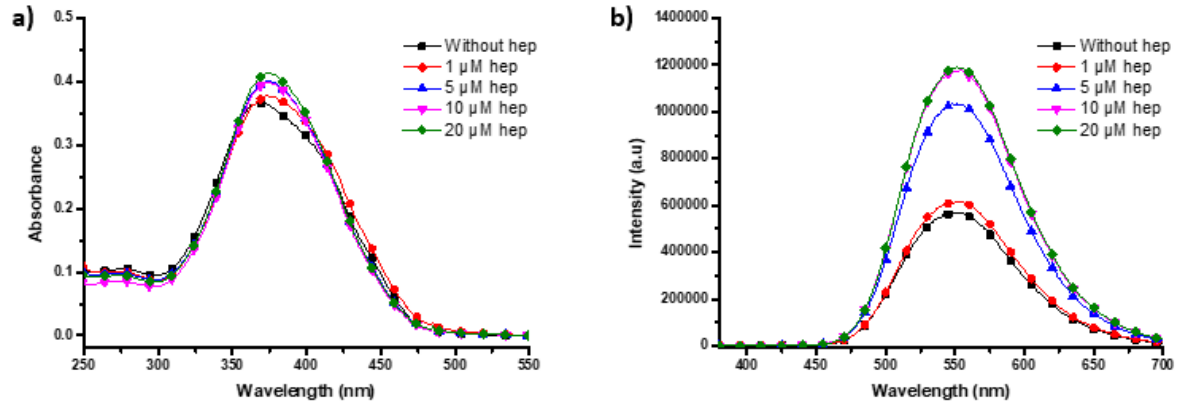

Fig. S7 (a) Absorption and (b) emission spectral changes **D*px*12** (5.0 μM) upon addition of different amount of heparin in aqueous buffer (5 mM tris-HCl, 99:1 water-DMSO).

Table S2 Fluorescence lifetime data of **D*px*N**s in presence of heparin in aqueous buffer (λ_{ex} = 340 nm).

D*px*N derivative	**λ_{em}**	**Lifetime (τ) parameters**	**Average lifetime (τ_{avg})**	**χ^2**
D*px*6 (5.0 µM) + Hep (10 µM)	540 nm	τ_1 = 3.35 ns (4%) τ_2 = 18.97 ns (96%)	18.34 ns	1.05
D*px*10 (5.0 µM) + Hep (10 µM)	545 nm	τ_1 = 4.51 ns (30%) τ_2 = 7.28 ns (6%) τ_2 = 13.05 ns (64%)	10.14 ns	1.07
D*px*12 (5.0 µM) + Hep (10 µM)	545 nm	τ_1 = 4.07 ns (15%) τ_2 = 11.10 ns (74%) τ_2 = 2.12 ns (11%)	9.06 ns	1.04

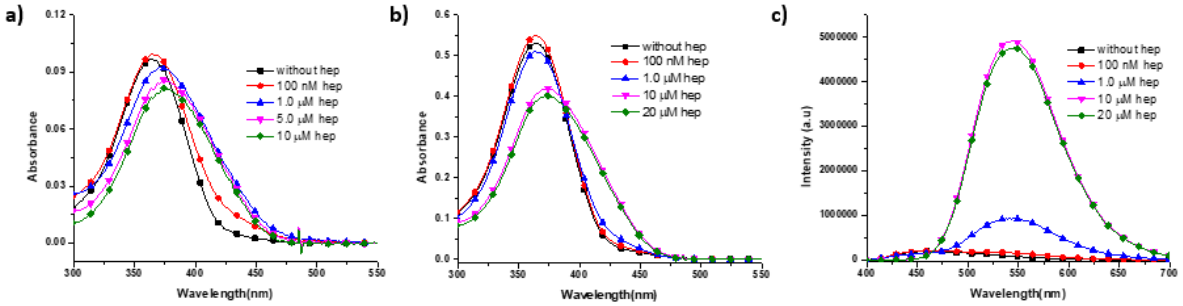

Fig. S8 Absorption spectral changes of **D*px*6** at (a) 1.0 µM and (b) 5.0 µM and (c) emission spectral changes of **D*px*6** (5.0 µM) upon addition of different amount of heparin in aqueous buffer (5 mM tris-HCl, 99:1 water-DMSO).

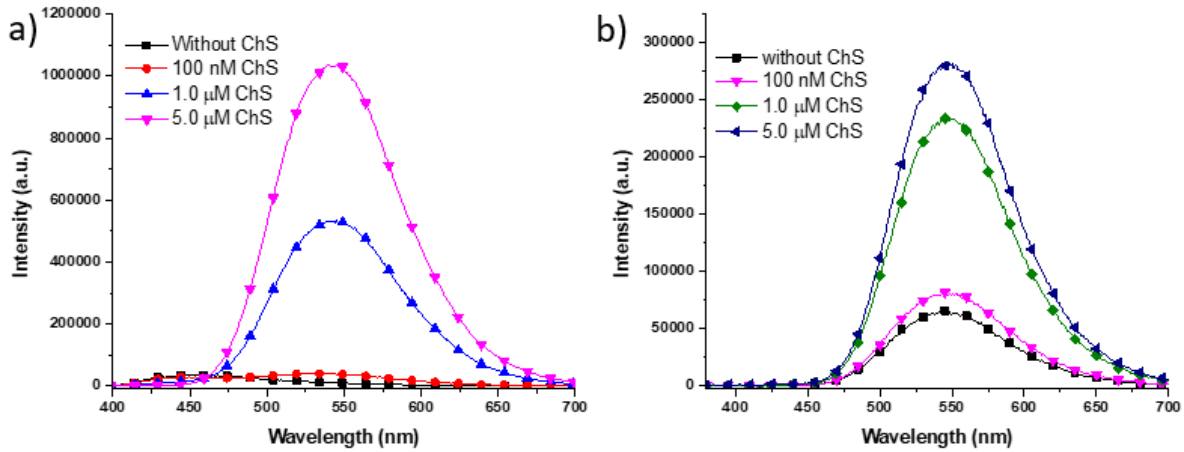

Fig. S9 Emission spectral changes of (a) **D*px*6** (1.0 μM) and (b) **D*px*10** (1.0 μM) upon addition of different amount of chondroitin sulfate (ChS) in aqueous buffer (5 mM tris-HCl, 99:1 water-DMSO).

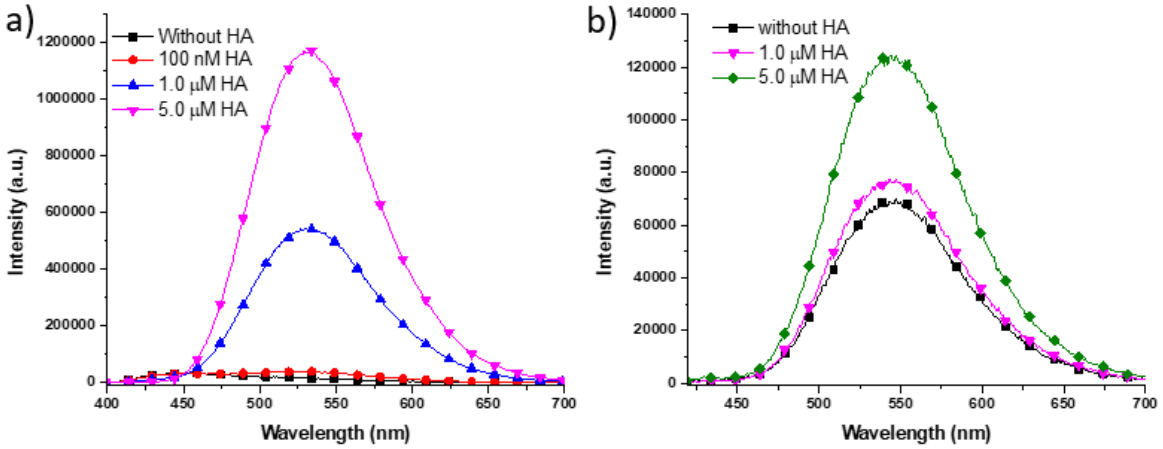

Fig. S10 Emission spectral changes of (a) **D*px*6** (1.0 μM) and (b) **D*px*10** (1.0 μM) upon addition of different amount of hyaluronic acid (HA) in aqueous buffer (5 mM tris-HCl, 99:1 water-DMSO).

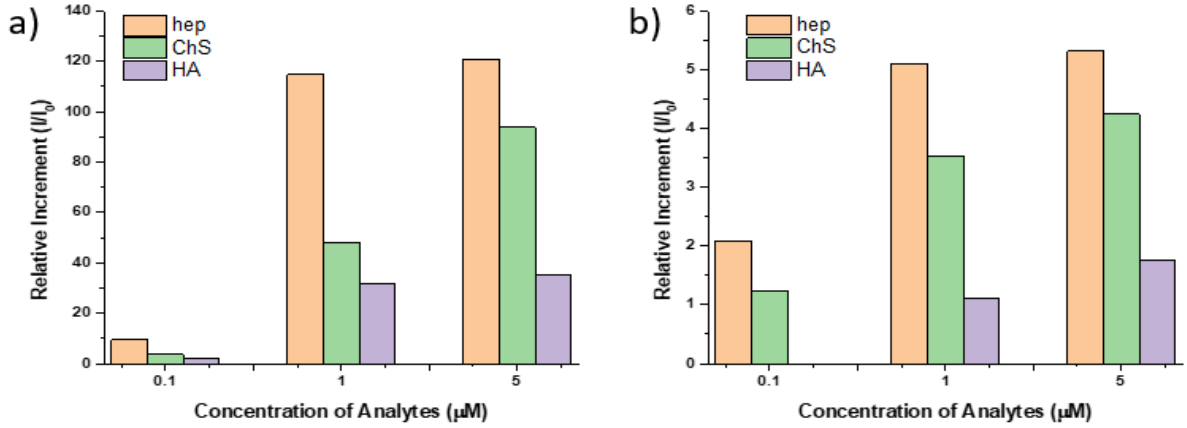

Fig. S11 Comparison bar diagram of (a) **D*px*6** (1.0 μM) and (b) **D*px*10** (1.0 μM) upon addition of heparin (hep), chondroitin sulfate (ChS) and hyaluronic acid (HA) in aqueous buffer (5 mM tris-HCl, 99:1 water-DMSO).

3. Heparin Binding Studies in Plasma and Serum

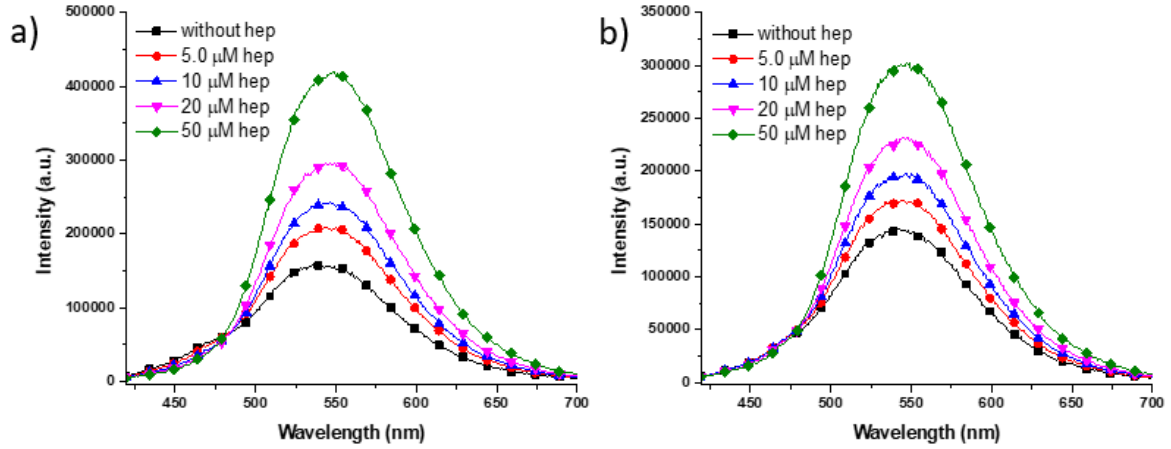

Fig. S12 Emission spectral changes of (a) **D*px*10** (25 μM) and (b) **D*px*12** (25 μM) upon addition of different amount of heparin in 25% plasma-aqueous buffer (5 mM tris-HCl, 99:1 water-DMSO).

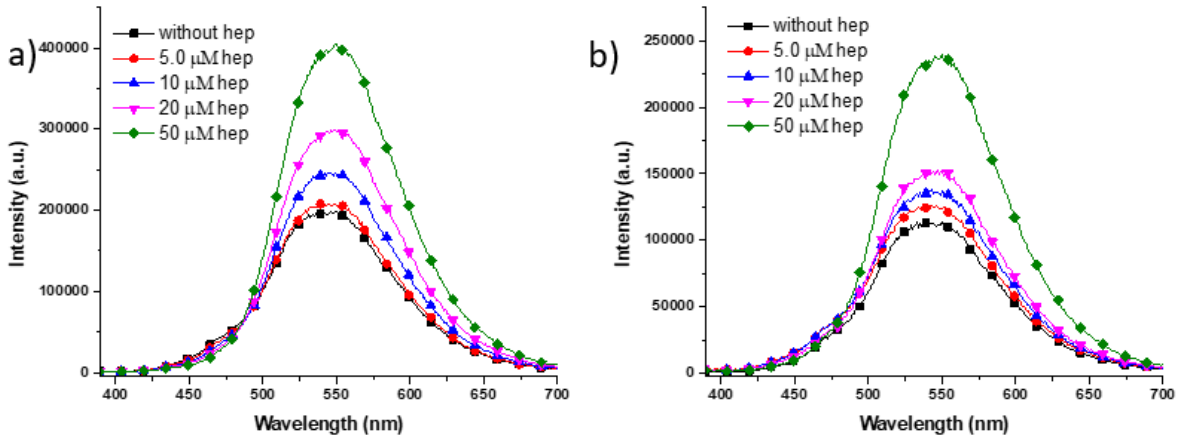

Fig. S13 Emission spectral changes of (a) **D*px*10** (30 μM) and (b) **D*px*12** (30 μM) upon addition of different amount of heparin in in 30% Serum-aqueous buffer (5 mM tris-HCl, 99:1 water-DMSO).

4. DNA Binding Studies in Buffer

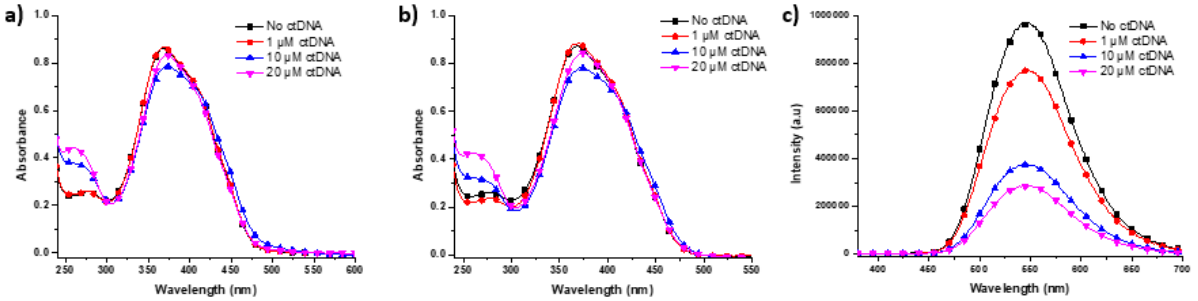

Fig. S14 Absorption spectral changes of (a) **D*px*10** (10.0 μM) and (b) **D*px*12** (10.0 μM), and (c) emission spectral changes of **D*px*10** (10.0 μM) upon addition of different amount of ctDNA in aqueous buffer (5 mM tris-HCl, 99:1 water-DMSO).

Table S3 DLS data for the average size and zeta potential (ζ) of **D*px*N** derivatives before and after ctDNA addition in aqueous buffer (5 mM tris-HCl, 99:1 water/DMSO, pH 7.4).

D*px*N derivatives	**Size w/o-ctDNA (nm)**	**Size w/- ctDNA (20 µM) (nm)**	**ζ w/o-ctDNA (mV)**	**ζ w/-ctDNA (20 µM) (mV)**
D*px*6 (10 µM)	95	1021	22.3	8.45
D*px*10 (10 µM)	204	272	31.6	-36.9
D*px*12 (10 µM)	164	261	27.8	-38.4

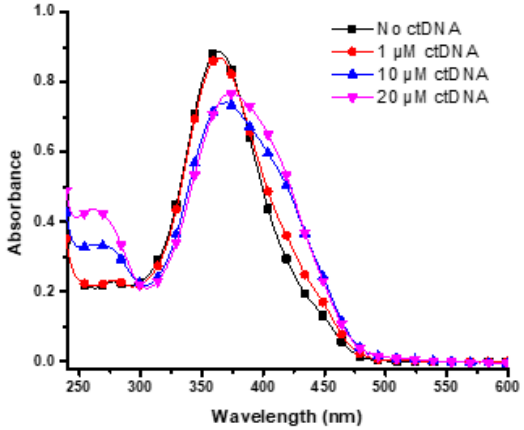

Fig. S15 Absorption spectral changes of **D*px*6** (10.0 µM) upon addition of different amount of ctDNA in aqueous buffer (5 mM tris-HCl, 99:1 water-DMSO).

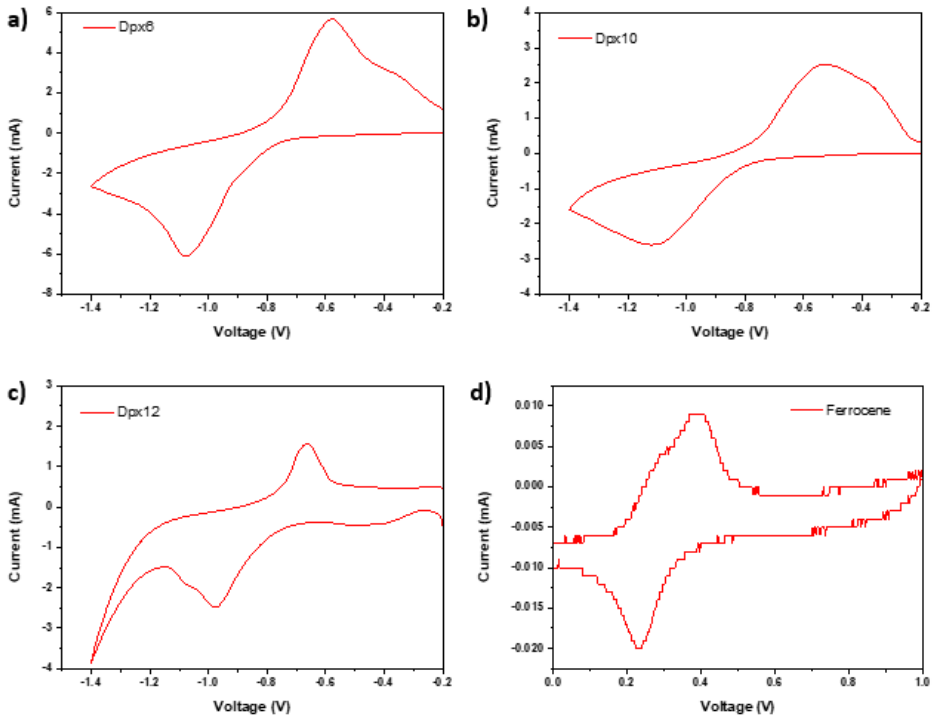

Fig. S16 Cyclic voltammograms of (a) **D*px*6**, (b) **D*px*10** and (c) **D*px*12** in film state on a carbon paper in 60% water-acetonitrile solvent. (d) Cyclic voltammogram of ferrocene as reference in the same medium. Working electrode: Carbon paper; Reference electrode: Ag/AgCl; Secondary electrode: Pt electrode; Electrolyte: 0.5M KCl.

HOMO energy calculation of $D_{px}N$ derivatives:

$E^{1/2}{}_{Fc/Fc^+}$= 0.31 V

(a) HOMO energy calculation for **D_{px}6**-

E_{red}^{onset} = -0.78 V, E_{LUMO} = - (E_{red}^{onset} – $E^{1/2}{}_{Fc/Fc^+}$ + 4.8 V) × e = -3.71 eV

Band gap energy = E_g = 1242/474 eV = 2.62 eV

E_{HOMO} = E_{LUMO} – E_g = -6.33 eV

(b) HOMO energy calculation for **D_{px}10**-

E_{red}^{onset} = -0.81 V, E_{LUMO} = - (E_{red}^{onset} – $E^{1/2}{}_{Fc/Fc^+}$ + 4.8 V) × e = -3.68 eV

Band gap energy = E_g = 1242/478 eV = 2.60 eV

E_{HOMO} = E_{LUMO} – E_g = -6.28 eV

(c) HOMO energy calculation for **D_{px}12**-

E_{red}^{onset} = -0.77 V, E_{LUMO} = - (E_{red}^{onset} – $E^{1/2}{}_{Fc/Fc^+}$ + 4.8 V) × e = -3.72 eV

Band gap energy = E_g = 1242/478 eV = 2.60 eV

E_{HOMO} = E_{LUMO} – E_g = -6.32 eV

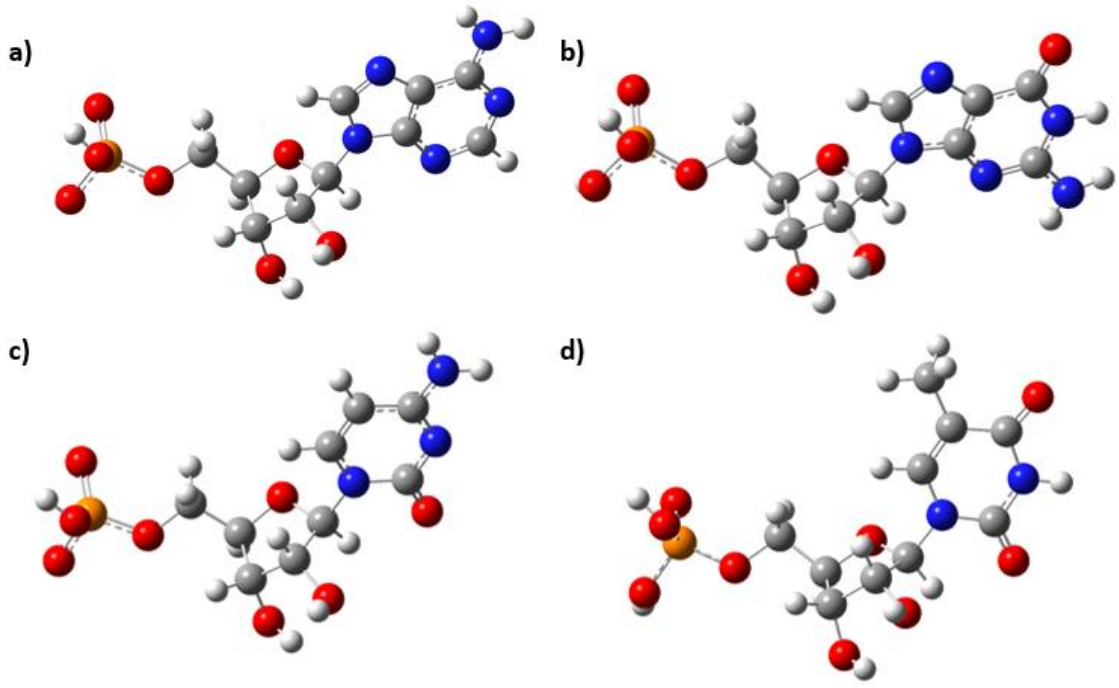

Fig. S17 DFT optimized structures of (a) adenosine monophosphate (AMP), (b) guanosine monophosphate (GMP), (c) cytidine monophosphate (CMP) and (d) thymidine monophosphate (TMP). Density functional theory (DFT) to optimize the structures were carried out using b3lyp/6-31+g(d,p) level of theory implying CPCM model with water as solvent.

Table S4 HOMO and LUMO energies of AMP, GMP, CMP and TMP calculated by DFT.

Nucleoside monophosphate	**HOMO (in a.u.)**	**HOMO (in eV)**	**LUMO (in a.u.)**	**LUMO (in eV)**
AMP	-0.23784	-6.47	-0.04277	-1.164
GMP	-0.22748	-6.19	-0.03119	-0.849
CMP	-0.24990	-6.80	-0.05286	-1.438
TMP	-0.25257	-6.87	-0.0576	-1.567

Table S5 Fluorescence lifetime data of **D*px*N**s in absence and presence of ctDNA in aqueous buffer (λ_{ex} = 340 nm).

D*px*N derivative	**λ_{em}**	**Lifetime (τ) parameters**	**Average lifetime (τ_{avg})**	**χ^2**
D*px*6 (10 µM)	545 nm	τ_1 = 1.93 ns (40%) τ_2 = 6.77 ns (56%) τ_3 = 0.18 ns (4%)	4.57 ns	1.21
D*px*6 (10 µM) + ctDNA (20 µM)	545 nm	τ_1 = 2.35 ns (31%) τ_2 = 8.59 ns (61%) τ_3 = 0.52 ns (8%)	6.01 ns	1.15
D*px*10 (10 µM)	545 nm	τ_1 = 1.61 ns (15%) τ_2 = 7.58 ns (85%)	6.69 ns	1.22
D*px*10 (10 µM) + ctDNA (20 µM)	545 nm	τ_1 = 1.91 ns (47%) τ_2 = 0.46 ns (11%) τ_3 = 5.75 ns (42%)	3.36 ns	1.18
D*px*12 (10 µM)	545 nm	τ_1 = 1.48 ns (15%) τ_2 = 7.72 ns (85%)	6.78 ns	1.20
D*px*12 (10 µM) + ctDNA (20 µM)	545 nm	τ_1 = 1.63 ns (38%) τ_2 = 0.34 ns (6%) τ_3= 5.33 ns (56%)	3.62 ns	1.15

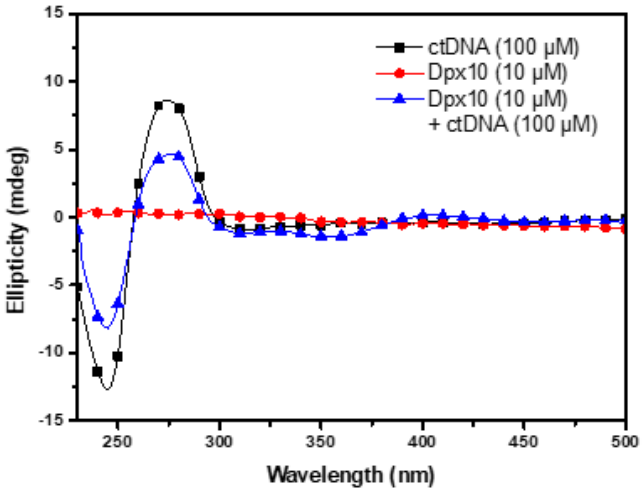

Fig. S18 CD spectra of **D$_{px}$10** (10.0 μM) in absence and presence of ctDNA (100 μM) in aqueous buffer (5 mM tris-HCl, 99:1 water-DMSO).

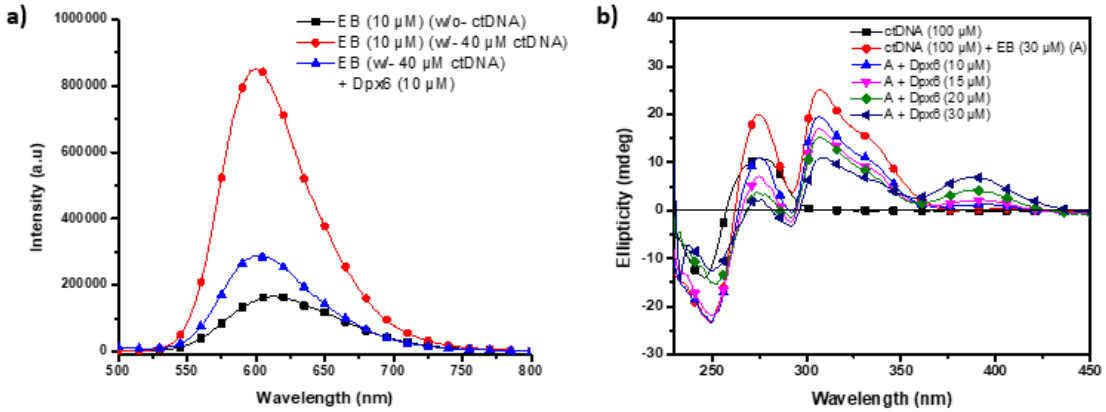

Fig. S19 (a) Emission spectral change of ctDNA-bound ethidium bromide (**EB**) (10 μM) upon addition of **D$_{px}$6** (10 μM) in buffer. (b) CD spectral changes of ctDNA-bound ethidium bromide (**EB**) (10 μM) upon addition of different amount of **D$_{px}$6** in buffer.

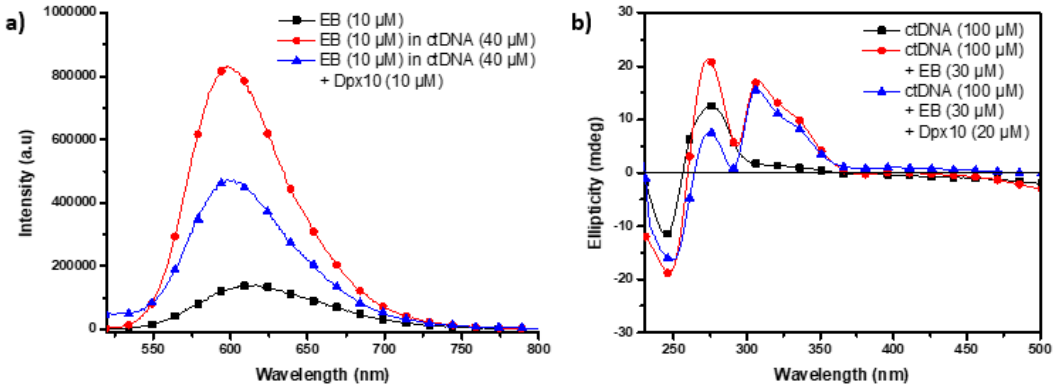

Fig. S20 (a) Emission spectral change of ctDNA-bound ethidium bromide (**EB**) (10 μM) upon addition of **D$_{px}$10** (10 μM) in buffer. (b) CD spectral change of ctDNA-bound ethidium bromide (**EB**) (10 μM) upon addition of **D$_{px}$10** (20 μM) in buffer.

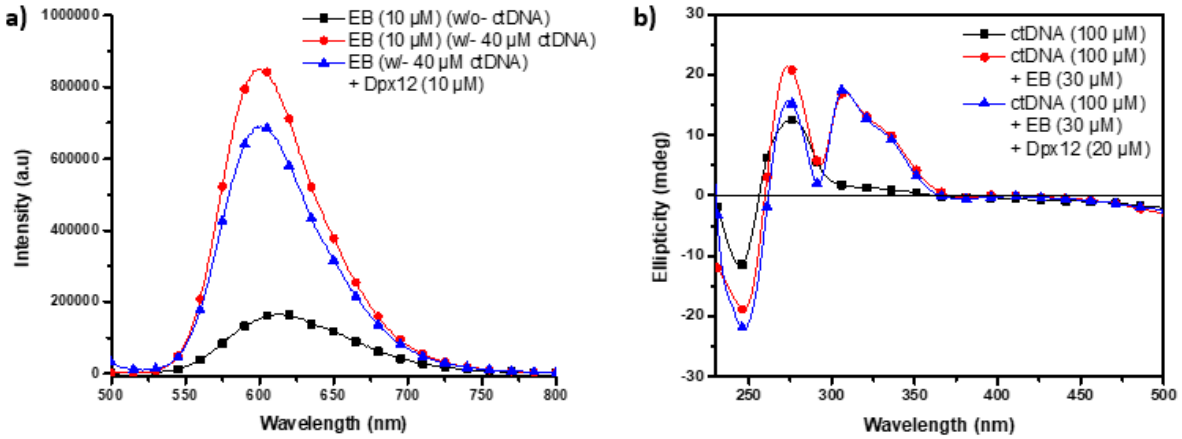

Fig. S21 (a) Emission spectral change of ctDNA-bound ethidium bromide (**EB**) (10 μM) upon addition of **D*px*12** (10 μM) in buffer. (b) CD spectral change of ctDNA-bound ethidium bromide (**EB**) (10 μM) upon addition of **D*px*12** (20 μM) in buffer.

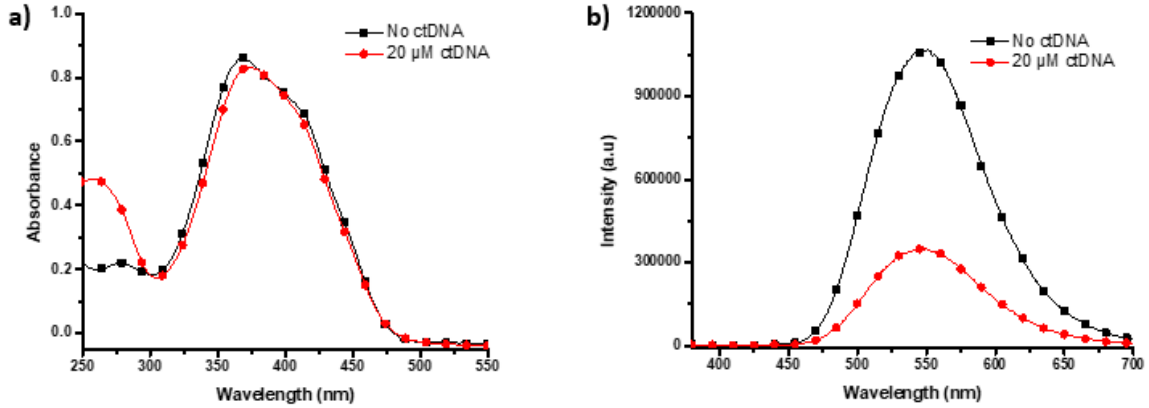

Fig. S22 (a) Absorption and (b) emission spectral changes of **D*px*10** (10 μM) in presence of ctDNA (20 μM) in buffer containing 2.5 mM NaCl.

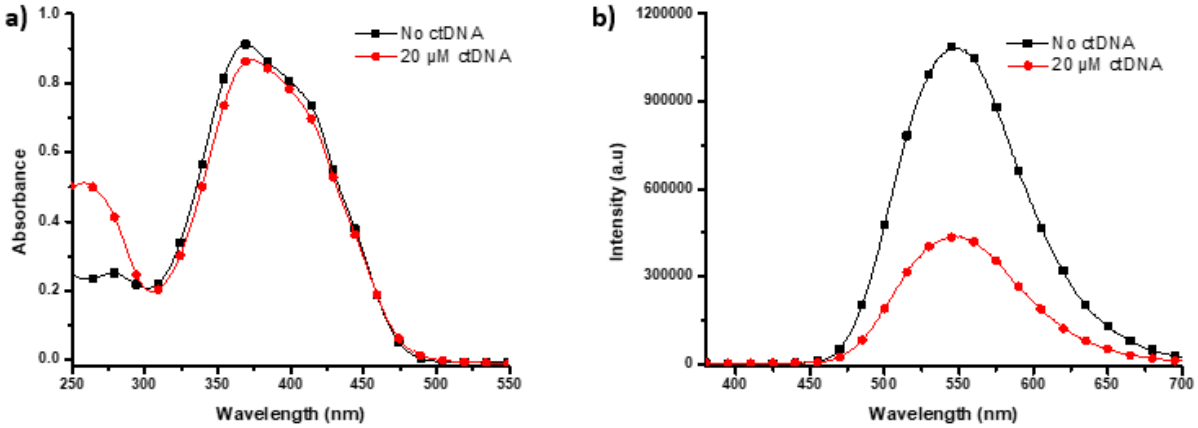

Fig. S23 (a) Absorption and (b) emission spectral changes of **D*px*10** (10 μM) in presence of ctDNA (20 μM) in buffer containing 5 mM NaCl.

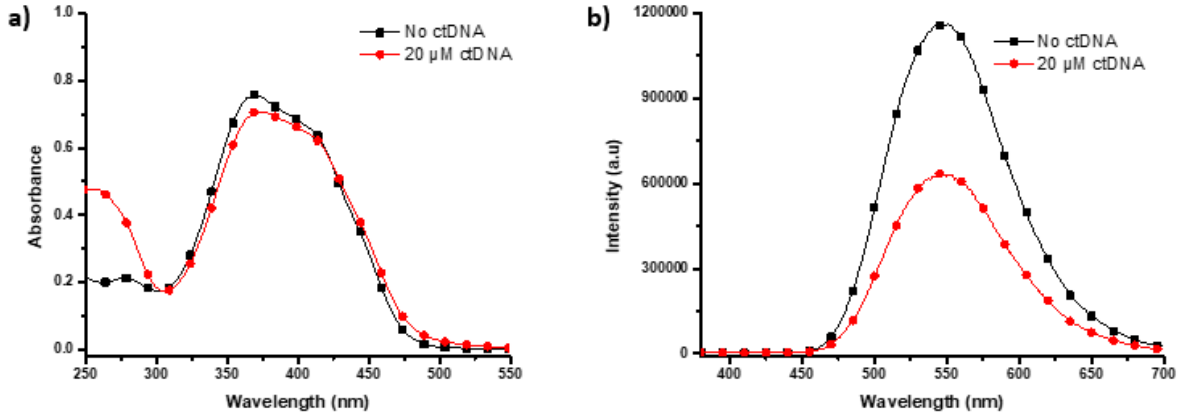

Fig. S24 (a) Absorption and (b) emission spectral changes of **D*px*10** (10 μM) in presence of ctDNA (20 μM) in buffer containing 10 mM NaCl.

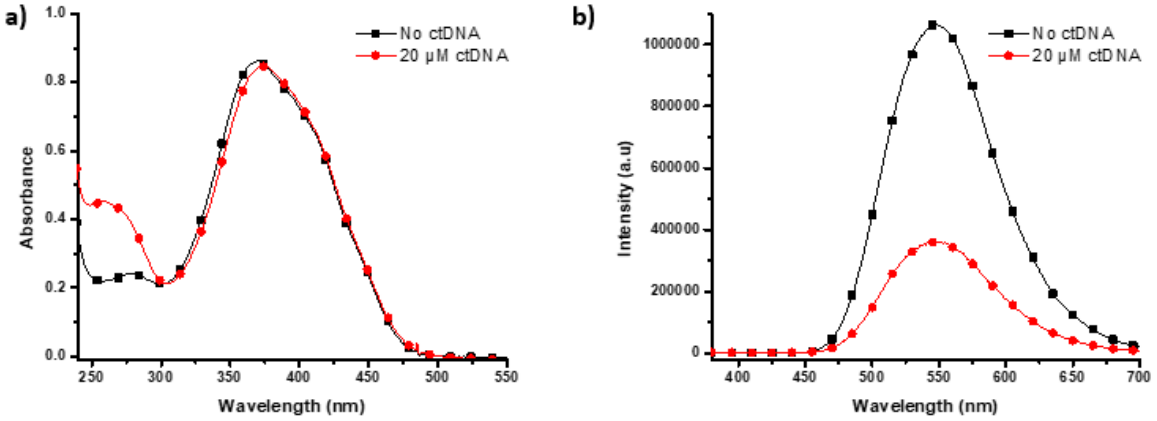

Fig. S25 (a) Absorption and (b) emission spectral changes of **D*px*12** (10 μM) in presence of ctDNA (20 μM) in buffer containing 2.5 mM NaCl.

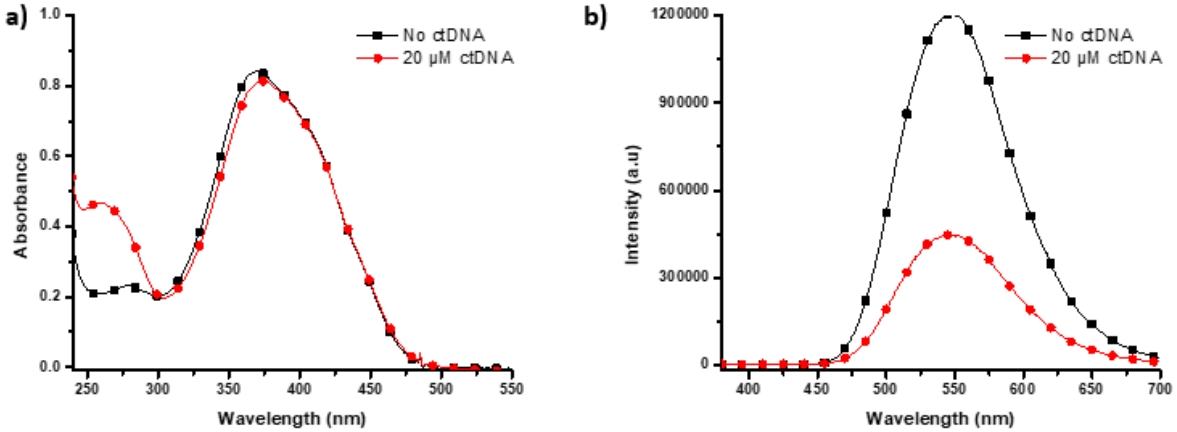

Fig. S26 (a) Absorption and (b) emission spectral changes of **D*px*12** (10 μM) in presence of ctDNA (20 μM) in buffer containing 5 mM NaCl.

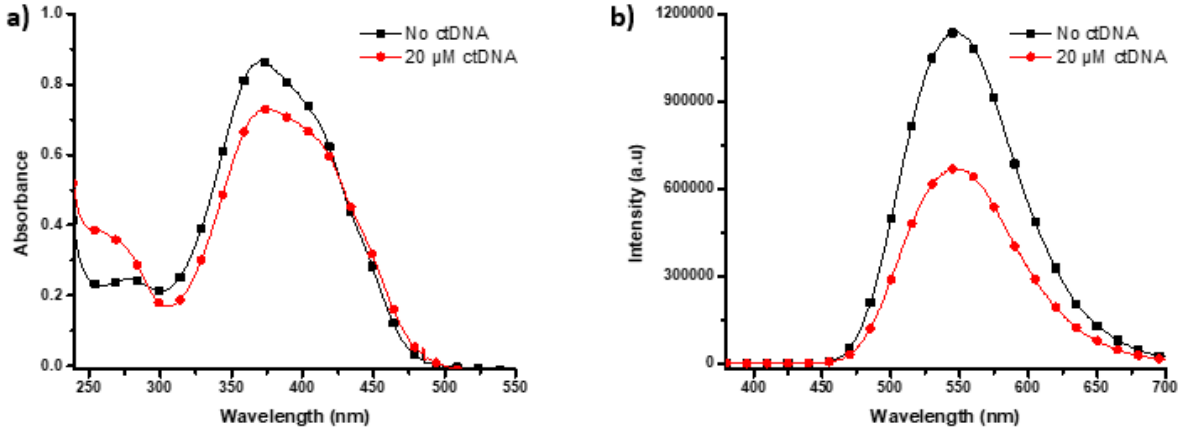

Fig. S27 (a) Absorption and (b) emission spectral changes of **D*px*12** (10 μM) in presence of ctDNA (20 μM) in buffer containing 10 mM NaCl.

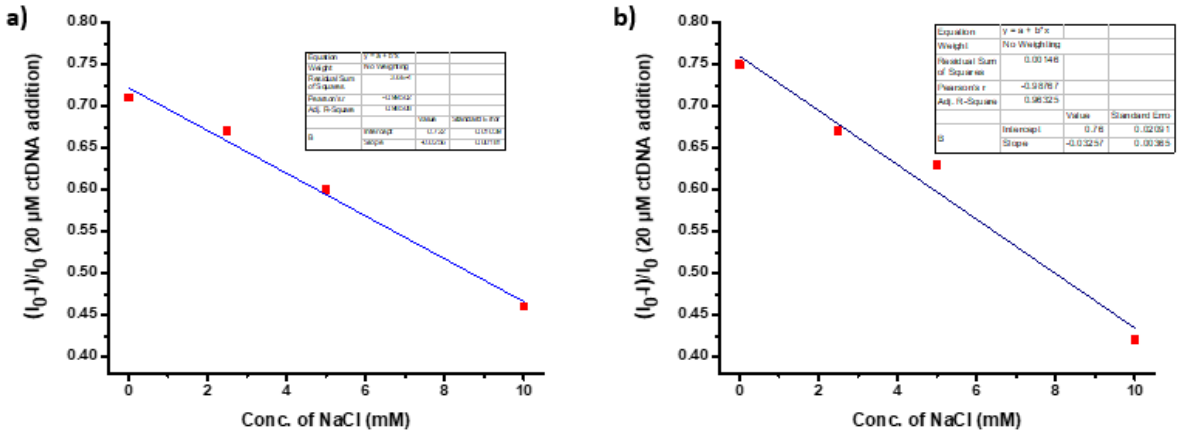

Fig. S28 Changes in $(I_0-I)/I_0$ (at 545 nm) of (a) **D*px*10** (10 μM) and (b) **D*px*12** (10 μM) in presence of ctDNA (20 μM) in buffer containing different amount of NaCl.

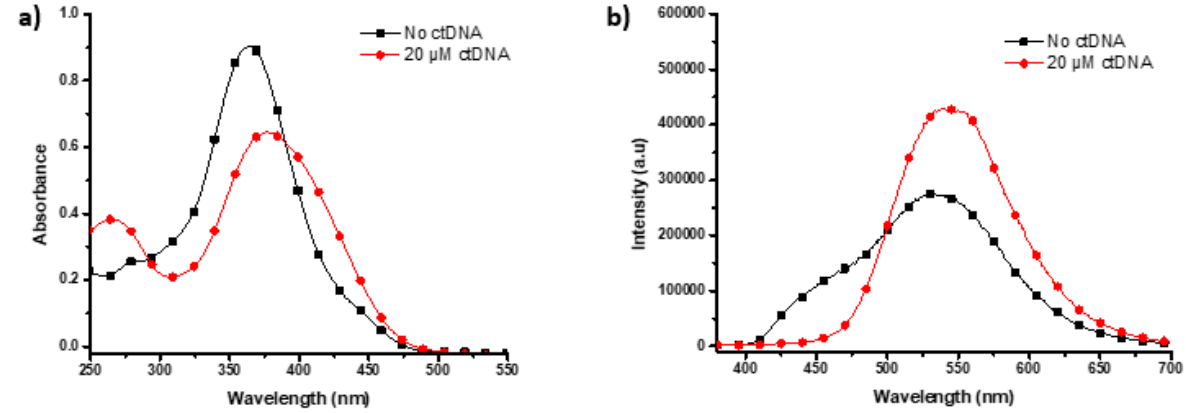

Fig. S29 (a) Absorption and (b) emission spectral changes of **D*px*6** (10 μM) in presence of ctDNA (20 μM) in buffer containing 2.5 mM NaCl.

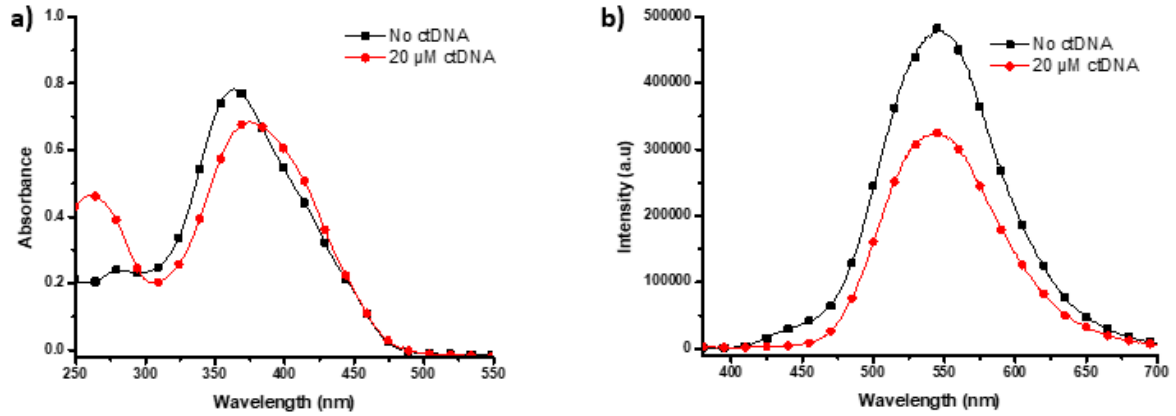

Fig. S30 (a) Absorption and (b) emission spectral changes of **D$_{px}$6** (10 μM) in presence of ctDNA (20 μM) in buffer containing 5 mM NaCl.

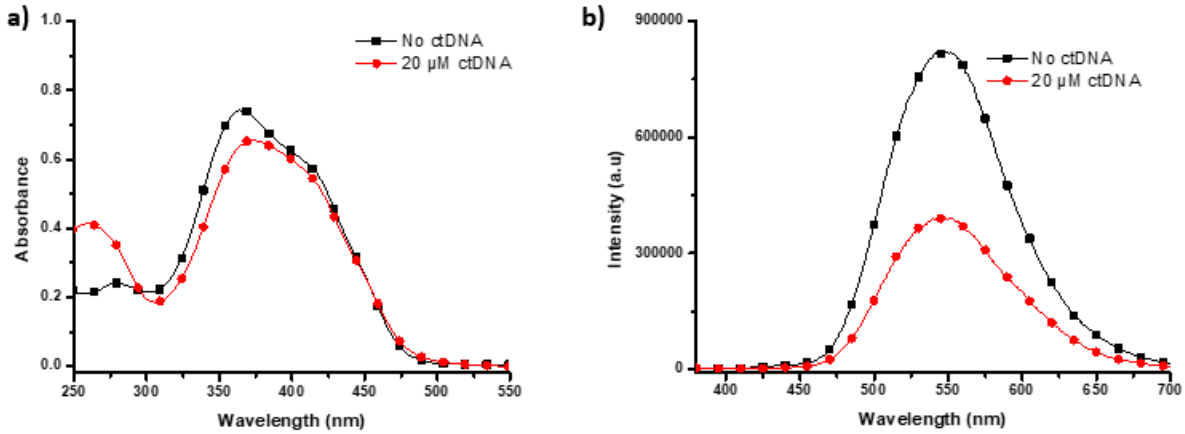

Fig. S31 (a) Absorption and (b) emission spectral changes of **D$_{px}$6** (10 μM) in presence of ctDNA (20 μM) in buffer containing 10 mM NaCl.

Table S6 Average size of **D$_{px}$6** (10 μM) in buffer and in buffer containing 10 mM NaCl as measured by DLS.

NaCl concentration in buffer	Size (nm)	KCPS
0 mM	95	164
10 mM	184	316

5. Energy Transfer Studies

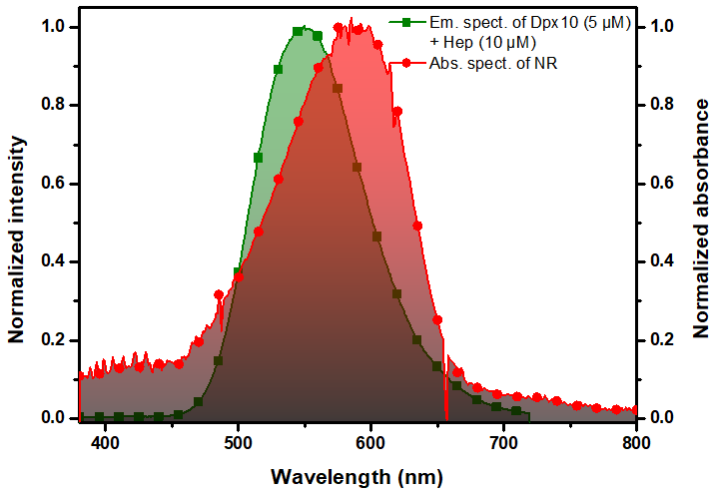

Overlay integral (*J*) between emission spectra of **D*px*10** (5 μM)-Hep (10 μM) and absorption spectra of Nile Red (**NR**) was calculated to be 9×10^{14} $nm^4M^{-1}cm^{-1}$. Calculation was done using FluorTools software.

Fig. S32 Normalized emission spectrum of **D*px*10** (5 μM)-Hep (10 μM) co-assembly and normalized absorption spectrum of Nile Red (**NR**).

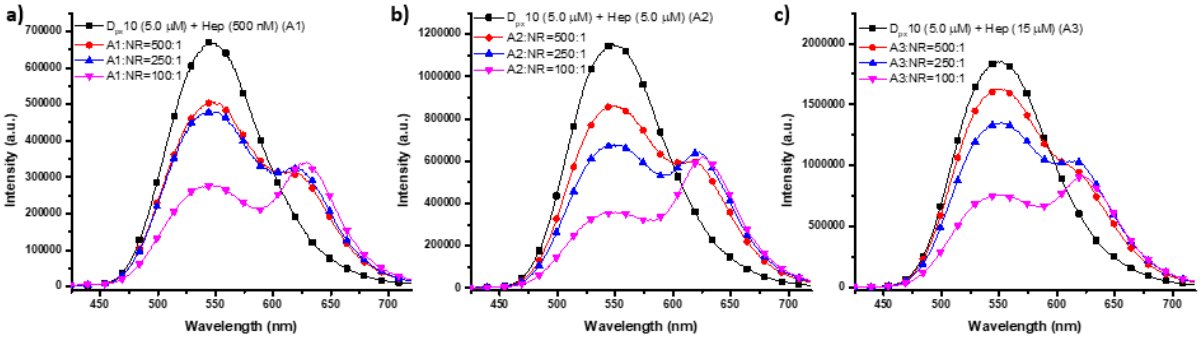

Fig. S33 Energy transfer from **D*px*10** (5.0 μM) to **NR** in presence of (a) 500 nM (b) 5.0 μM and (c) 15 μM Heparin in aqueous buffer.

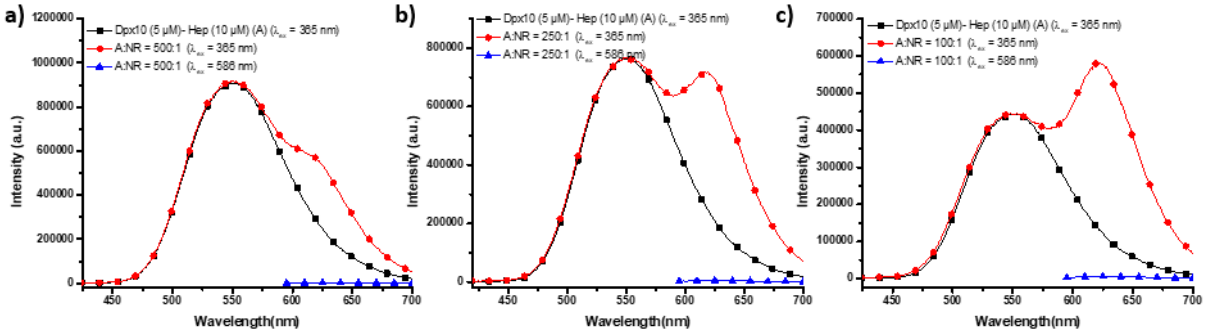

Fig. S34 Emission spectra of **D*px*10** (5.0 μM)-heparin (10 μM) (**A**)-**NR** in aqueous buffer. Red trace (donor emission, λ_{ex} = 365 nm) and blue trace (acceptor emission, λ_{ex} = 586 nm). Black trace represents emission spectrum of **D*px*10** (5.0 μM)-heparin (10 μM) (**A**) (λ_{ex} = 365 nm) which was normalized to the intensity at 545 nm of the red trace.

Table S7 ET efficiency (%) of **D*px*10**-Hep co-assemblies having different concentration of heparin in presence of Nile Red (**NR**) at different donor/acceptor ratio.

Donor/acceptor ratio	D_{px}10 (5 µM)-heparin (500 nM µM) (A1)	D_{px}10 (5 µM)-heparin (5 µM µM) (A2)	D_{px}10 (5 µM)-heparin (10 µM µM) (A)	D_{px}10 (5 µM)-heparin (15 µM µM) (A3)
500:1	25	26	36	12
250:1	28	41	50	27
100:1	58	69	69	59

Table S8 Antenna effect (AE) values of **D*px*10**-Hep co-assemblies having different concentration of heparin in presence of Nile Red (**NR**) at different donor/acceptor ratio.

Donor/acceptor ratio	D_{px}10 (5 µM)-heparin (500 nM µM) (A1)	D_{px}10 (5 µM)-heparin (5 µM µM) (A2)	D_{px}10 (5 µM)-heparin (10 µM µM) (A)	D_{px}10 (5 µM)-heparin (15 µM µM) (A3)
500:1	67	93	110	12
250:1	79	80	98	27
100:1	39	61	73	59

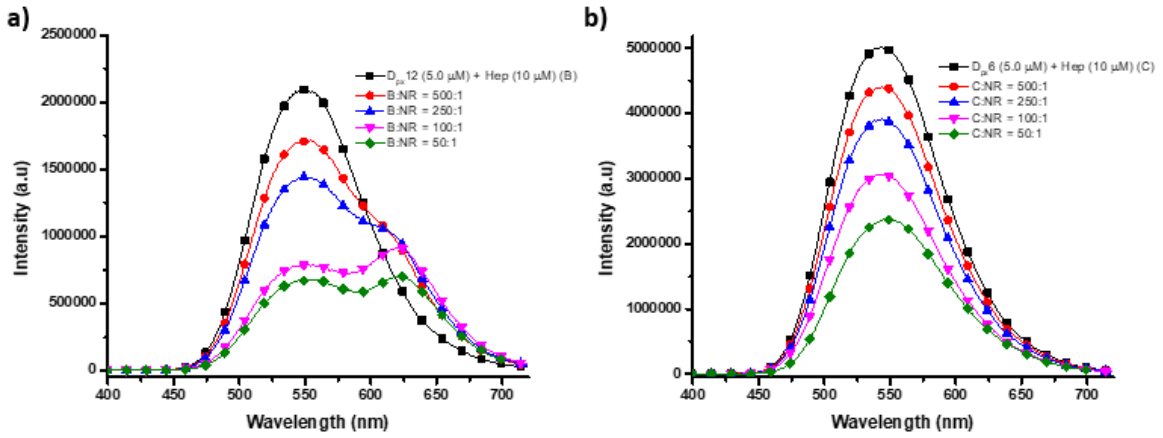

Fig. S35 Energy transfer from (a) **D_{px}12** (5.0 µM)-Hep (10 µM) (**B**) and (b) **D_{px}6** (5.0 µM)-Hep (10 µM) (**C**) to **NR** at different donor-acceptor ratio in aqueous buffer.

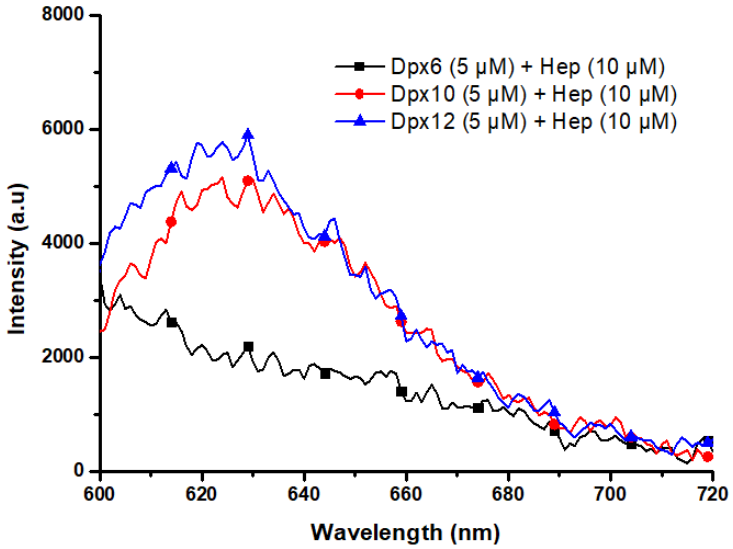

Fig. S36 Emission spectra of Nile Red (**NR**) (20 nM) in presence of different co-assemblies in aqueous buffer. (λ_{ex} = 586 nm)

Table S9 Steady-state emission anisotropy values (**r**) of Nile Red (**NR**) at 625 nm (λ_{ex} = 586 nm) in presence of **D*px*N** (5.0 μM)-heparin (10 μM) co-assemblies in aqueous buffer

Conc. of NR	**In aqueous buffer**	**In presence of D*px*6 (5 μM)-Hep (10 μM)**	**In presence of D*px*10 (5 μM)-Hep (10 μM)**	**In presence of D*px*12 (5 μM)-Hep (10 μM)**
50 nM	0.066	0.110	0.224	0.253

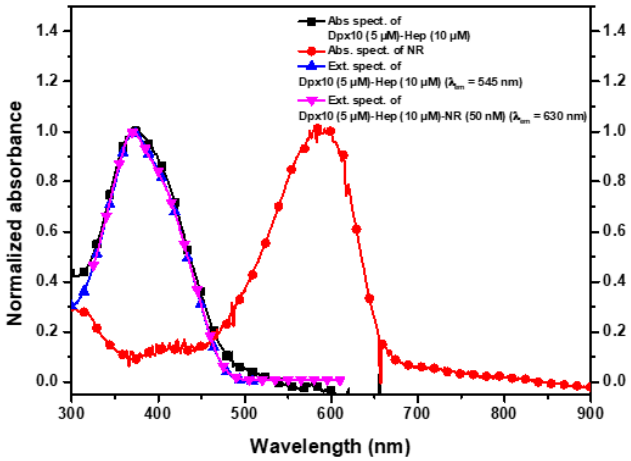

Fig. S37 Normalized absorption spectra of **D*px*10** (5 μM)-Heparin (10 μM), Nile Red (**NR**) and normalized excitation spectra of **D*px*10** (5 μM)-Heparin (10 μM) without Nile Red (**NR**) (λ_{em} = 545 nm) and with Nile Red (**NR**) (50 nM) (λ_{em} = 630 nm) in aqueous buffer.

Table S10 ET efficiency (%) of **D*px*N**-Hep co-assemblies in presence of Nile Red (**NR**) at different donor/acceptor ratio.

Donor/acceptor ratio	**D$_{px}$10 (5 µM)-heparin (10 µM) (A)**	**D$_{px}$12 (5 µM)-heparin (10 µM) (B)**	**D$_{px}$6 (5 µM)-heparin (10 µM) (C)**
500:1	36	18	12
250:1	50	32	23
100:1	69	63	39
50:1	73	68	53

Table S11 Antenna effect (AE) values of **D*px*N**-Hep co-assemblies in presence of Nile Red (**NR**) at different donor/acceptor ratio.

Donor/acceptor ratio	**D$_{px}$10 (5 µM)-heparin (10 µM) (A)**	**D$_{px}$12 (5 µM)-heparin (10 µM) (B)**	**D$_{px}$6 (5 µM)-heparin (10 µM) (C)**
500:1	110	87	6
250:1	98	89	5.9
100:1	73	79	2
50:1	44	50	19

Table S12 Average lifetimes (τ_{avg}) of **D$_{px}$N** (5 µM)-Hep (10 µM) co-assemblies without and with Nile Red (**NR**) in aqueous buffer.

Amount of NR	**Average lifetime (τ_{avg})**		
	D$_{px}$6 (5 µM)-Hep (10 µM)	**D$_{px}$10 (5 µM)-Hep (10 µM)**	**D$_{px12}$ (5 µM)-Hep (10 µM)**
Without	18.14 ns	10.34 ns	9.06 ns
50 nM	14.6 ns	6.48 ns	5.72 ns

6. Hydrodynamic Diameter Measurements

A. Size measurement of only D_{px}Ns:

I. D_{px}6 (10 µM) in buffer

Results

			Size (d.nm):	% Intensity:	St Dev (d.n...
Z-Average (d.nm):	94.84	Peak 1:	115.9	94.1	62.07
PdI:	0.342	Peak 2:	3868	5.9	1247
Intercept:	0.866	Peak 3:	0.000	0.0	0.000

Result quality : Refer to quality report

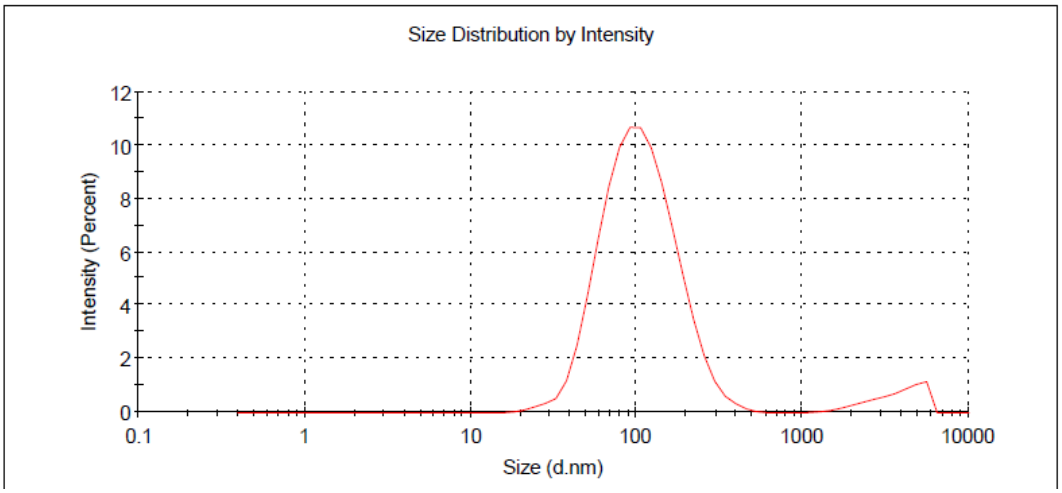

II. D_{px}6 (10 µM) in buffer containing 10 mM NaCl

Results

			Size (d.nm):	% Intensity:	St Dev (d.n...
Z-Average (d.nm):	183.5	Peak 1:	421.4	98.9	465.5
PdI:	0.496	Peak 2:	4626	1.1	735.9
Intercept:	0.927	Peak 3:	0.000	0.0	0.000

Result quality : Good

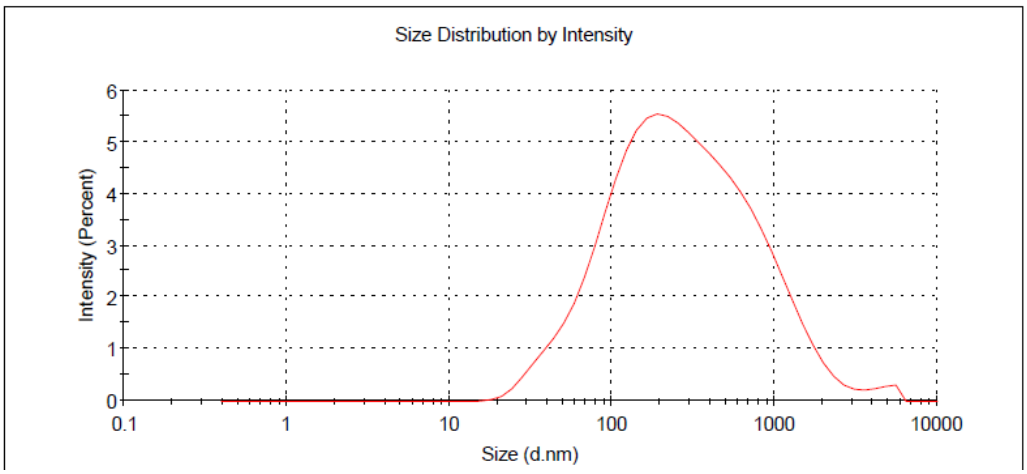

III. $D_{px}10$ (5 µM) in buffer

Results

			Size (d.nm):	% Intensity:	St Dev (d.n...
Z-Average (d.nm):	129.4	Peak 1:	168.5	100.0	89.00
PdI:	0.221	Peak 2:	0.000	0.0	0.000
Intercept:	0.948	Peak 3:	0.000	0.0	0.000
Result quality :	Good				

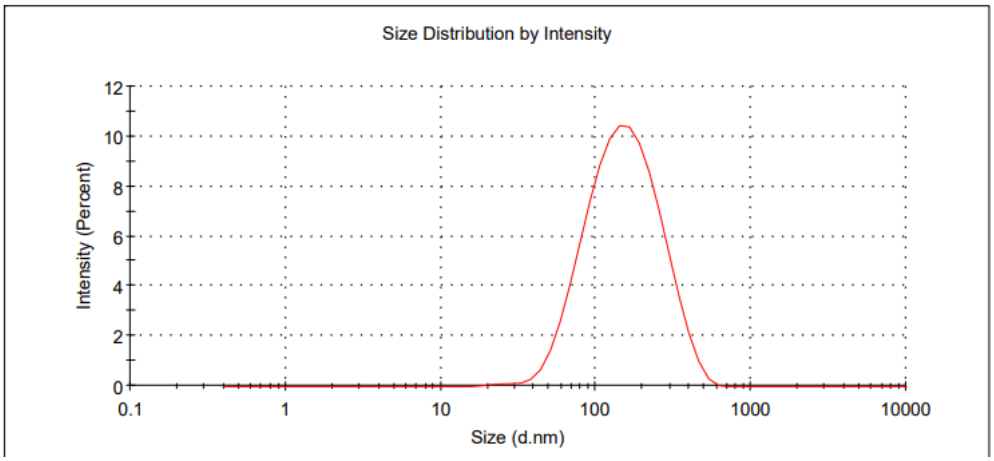

IV. $D_{px}10$ (1 µM) in buffer

Results

			Size (d.nm):	% Intensity:	St Dev (d.n...
Z-Average (d.nm):	109.6	Peak 1:	148.4	95.5	107.5
PdI:	0.298	Peak 2:	3862	3.6	1210
Intercept:	0.881	Peak 3:	21.64	0.9	3.797
Result quality :	Good				

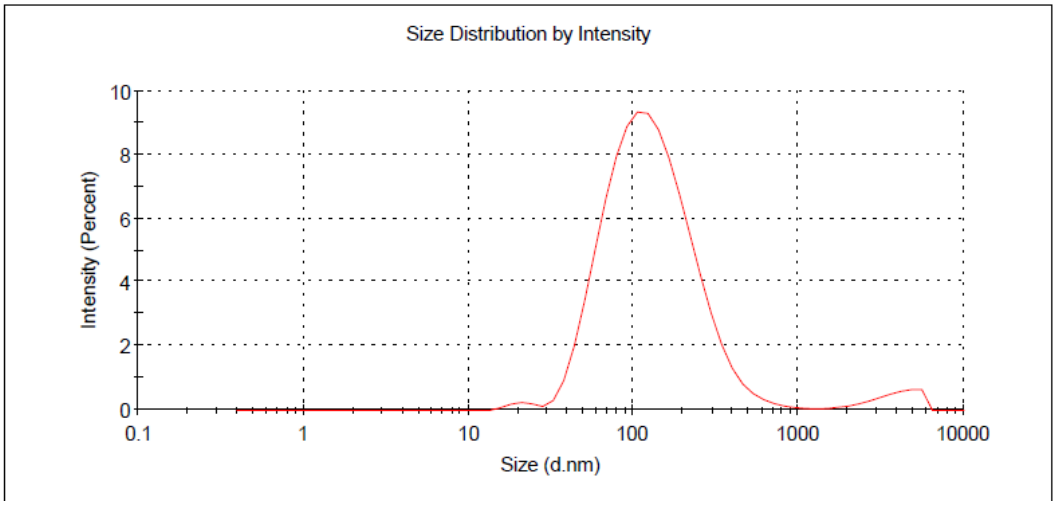

V. $D_{px}10$ (10 µM) in buffer

Results

		Size (d.nm):	% Intensity:	St Dev (d.n...
Z-Average (d.nm): 204.3	Peak 1:	289.1	99.6	173.7
PdI: 0.349	Peak 2:	5152	0.4	507.7
Intercept: 0.952	Peak 3:	0.000	0.0	0.000

Result quality : Good

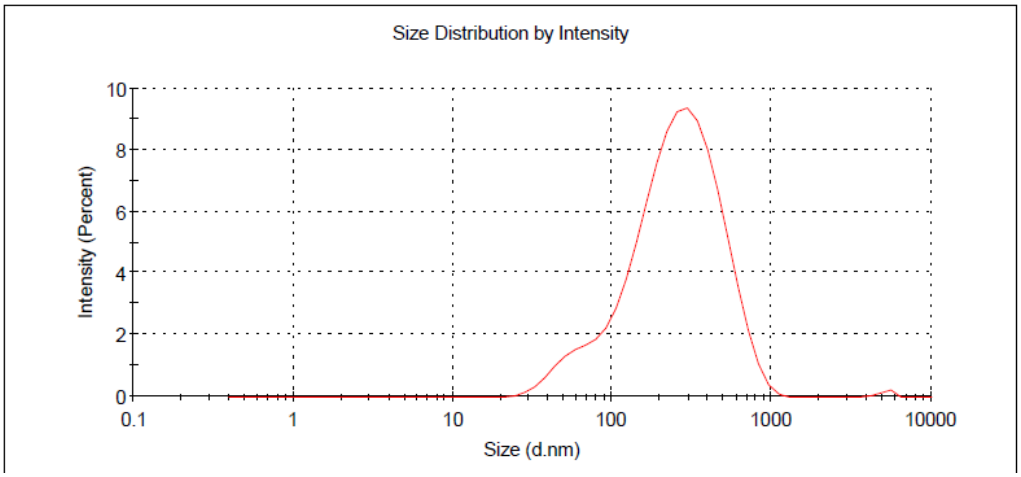

VI. $D_{px}12$ (5 µM) in buffer

Results

		Size (d.nm):	% Intensity:	St Dev (d.n...
Z-Average (d.nm): 133.1	Peak 1:	164.1	99.6	75.46
PdI: 0.214	Peak 2:	5200	0.4	474.5
Intercept: 0.950	Peak 3:	0.000	0.0	0.000

Result quality : Good

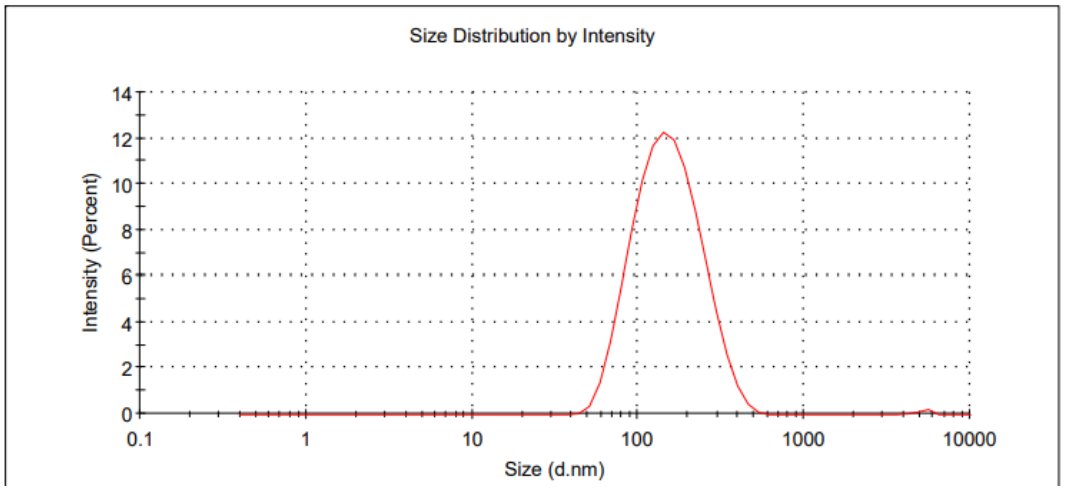

VII. $D_{px}12$ (1 µM) in buffer

Results

		Size (d.nm):	% Intensity:	St Dev (d.n...
Z-Average (d.nm): 96.98	Peak 1:	127.0	99.6	68.32
PdI: 0.232	Peak 2:	4912	0.4	663.0
Intercept: 0.890	Peak 3:	0.000	0.0	0.000

Result quality : Good

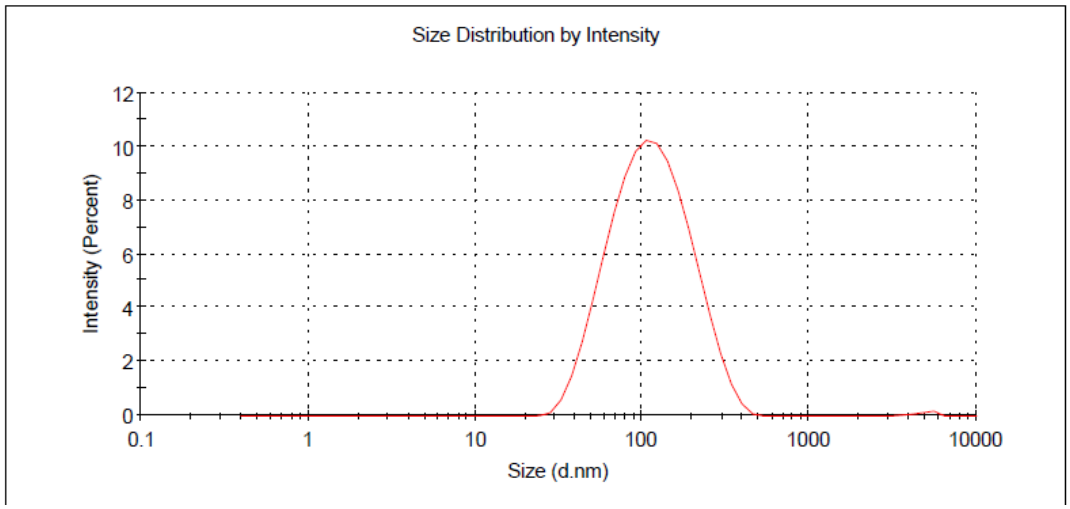

VIII. $D_{px}12$ (10 µM) in buffer

Results

		Size (d.nm):	% Intensity:	St Dev (d.n...
Z-Average (d.nm): 164.2	Peak 1:	203.0	99.6	92.32
PdI: 0.181	Peak 2:	31.17	0.4	4.767
Intercept: 0.947	Peak 3:	0.000	0.0	0.000

Result quality : Good

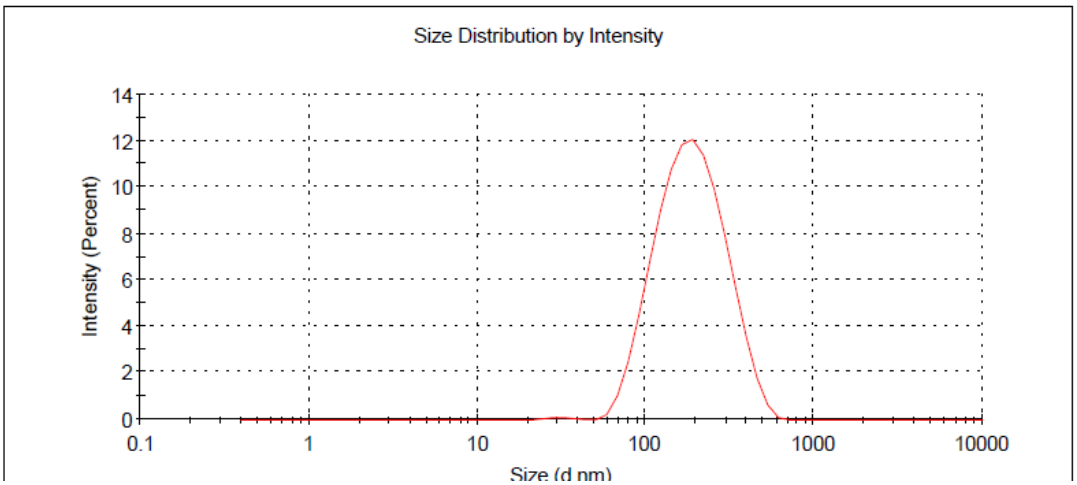

B. Size measurement of D_{px}N-heparin co-assemblies:

A. D_{px}6 (5 μM)-heparin (10 μM) in buffer

Results

			Size (d.nm):	% Intensity:	St Dev (d.n...
Z-Average (d.nm):	73.42	Peak 1:	90.91	96.0	43.15
PdI:	0.290	Peak 2:	4966	2.1	685.1
Intercept:	0.811	Peak 3:	15.33	1.9	3.006
Result quality :	Good				

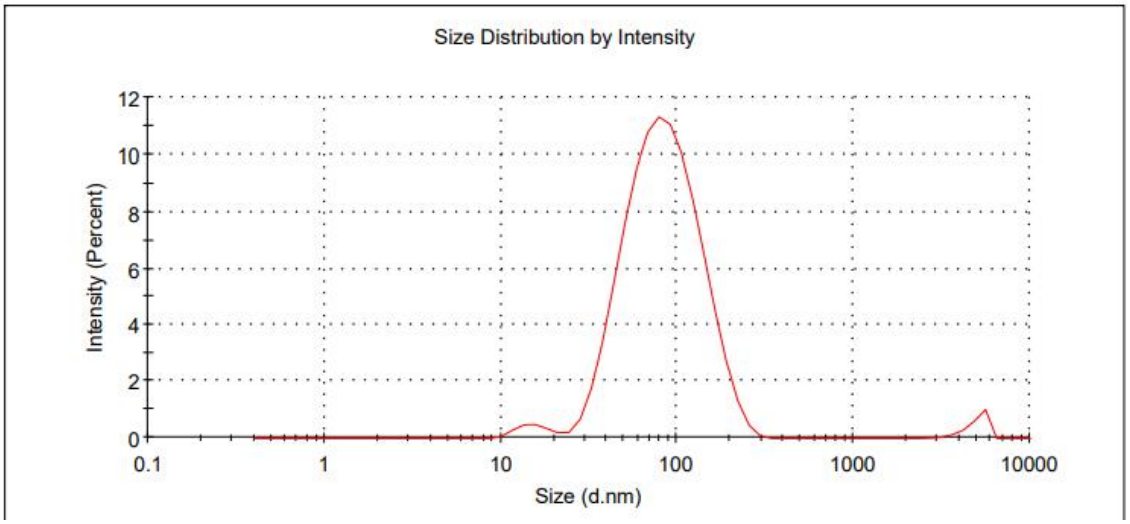

B. D_{px}10 (5 μM)-heparin (10 μM) in buffer

Results

			Size (d.nm):	% Intensity:	St Dev (d.n...
Z-Average (d.nm):	124.6	Peak 1:	151.0	99.1	72.20
PdI:	0.204	Peak 2:	4845	0.9	703.5
Intercept:	0.954	Peak 3:	0.000	0.0	0.000
Result quality :	Good				

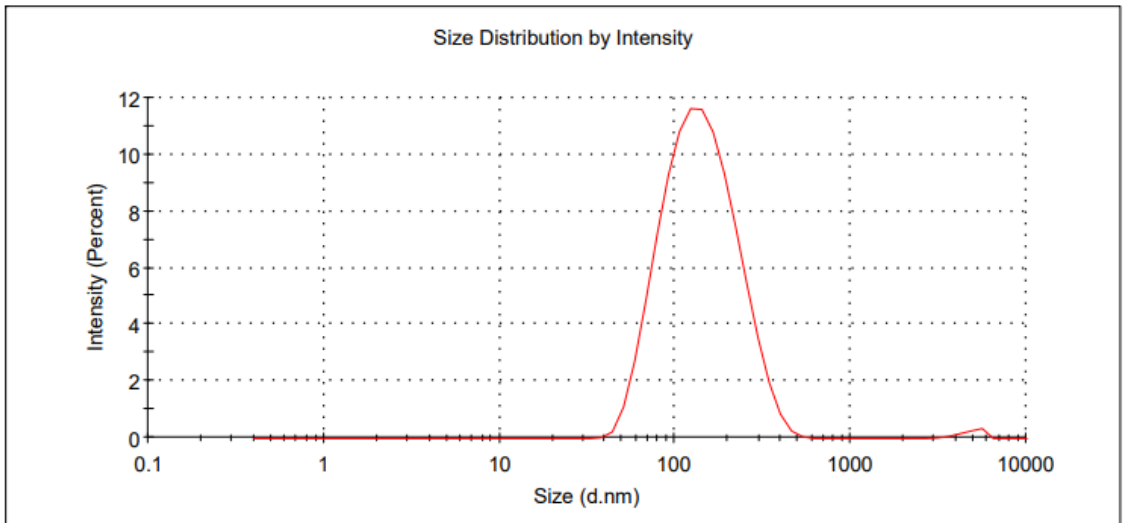

C. D$_{px}$10 (1 µM)-heparin (2 µM) in buffer

Results

		Size (d.nm):	% Intensity:	St Dev (d.n...
Z-Average (d.nm): 110.7	Peak 1:	130.3	96.8	64.43
PdI: 0.273	Peak 2:	4806	3.2	746.3
Intercept: 0.938	Peak 3:	0.000	0.0	0.000

Result quality : Good

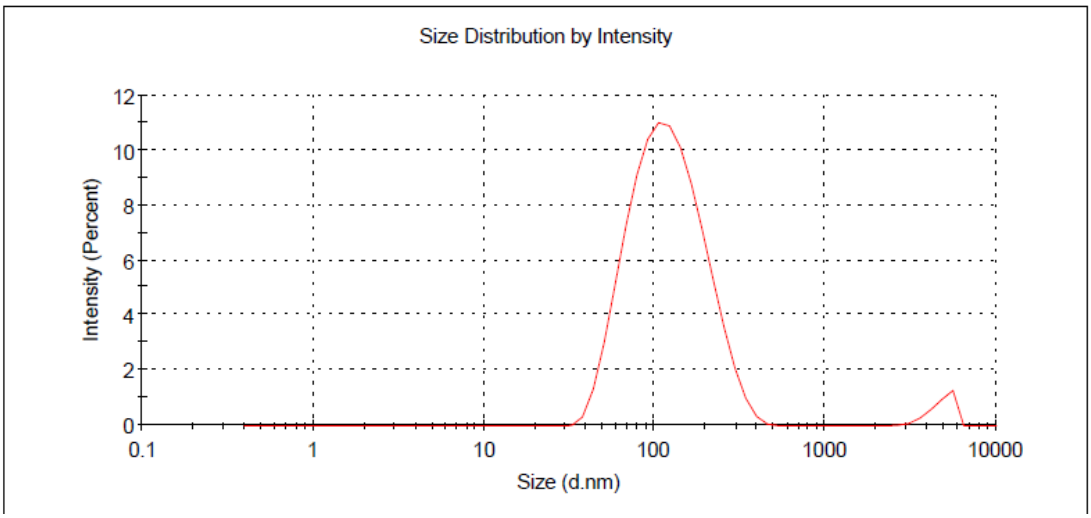

D. D$_{px}$12 (5 µM)-heparin (10 µM) in buffer

Results

		Size (d.nm):	% Intensity:	St Dev (d.n...
Z-Average (d.nm): 131.3	Peak 1:	167.6	100.0	83.65
PdI: 0.214	Peak 2:	0.000	0.0	0.000
Intercept: 0.950	Peak 3:	0.000	0.0	0.000

Result quality : Good

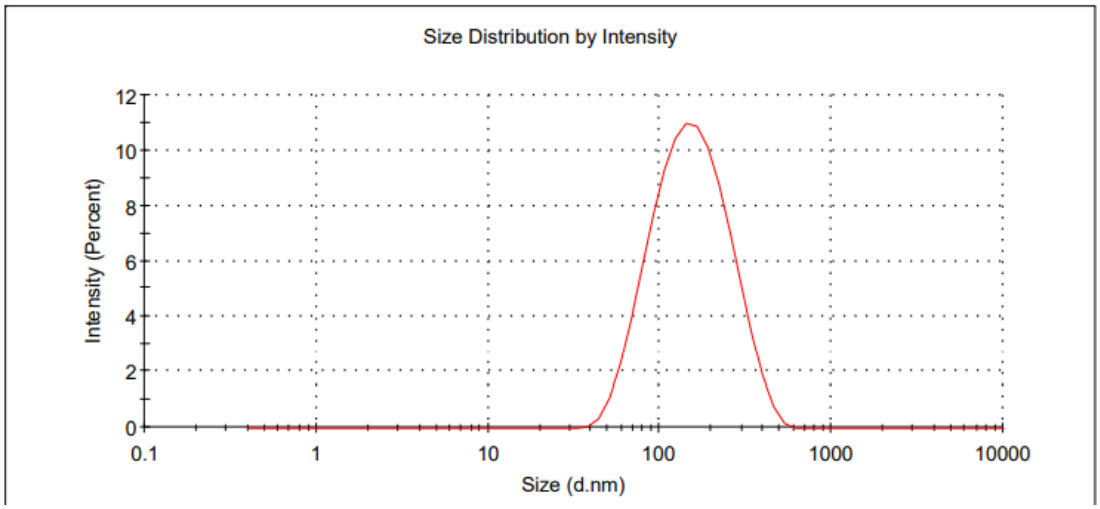

E. $D_{px}12$ (1 µM)-heparin (2 µM) in buffer

Results

		Size (d.nm):	% Intensity:	St Dev (d.n...
Z-Average (d.nm): 104.5	Peak 1:	132.1	95.9	66.54
PdI: 0.289	Peak 2:	4720	2.2	824.5
Intercept: 0.925	Peak 3:	23.73	1.9	3.639

Result quality : Good

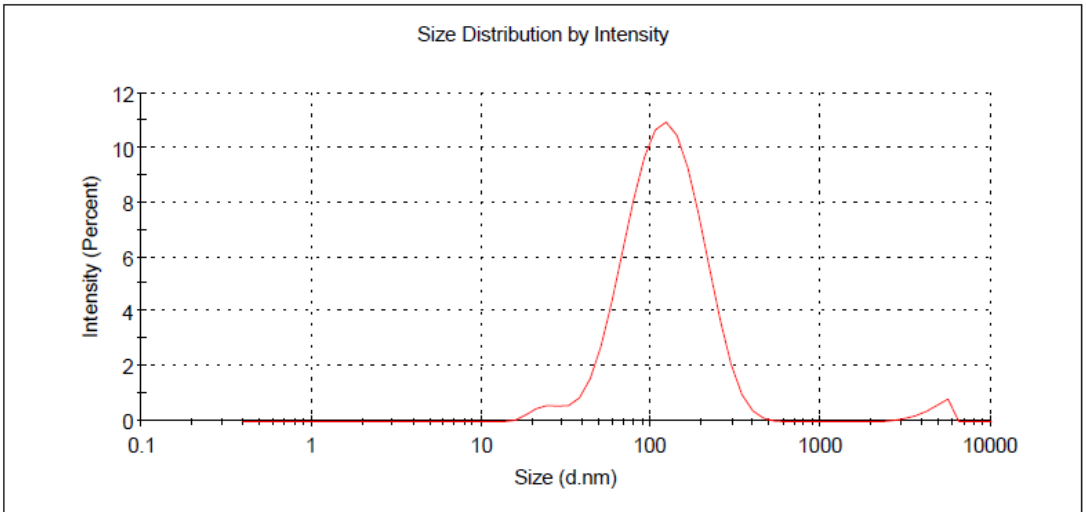

C. Size measurement of D_{px}N-ctDNA co-assemblies:

I. $D_{px}6$ (10 µM)-ctDNA (20 µM) in buffer

Results

		Size (d.nm):	% Intensity:	St Dev (d.n...
Z-Average (d.nm): 1021	Peak 1:	1620	97.6	1049
PdI: 0.453	Peak 2:	147.1	2.4	26.70
Intercept: 0.971	Peak 3:	0.000	0.0	0.000

Result quality : Good

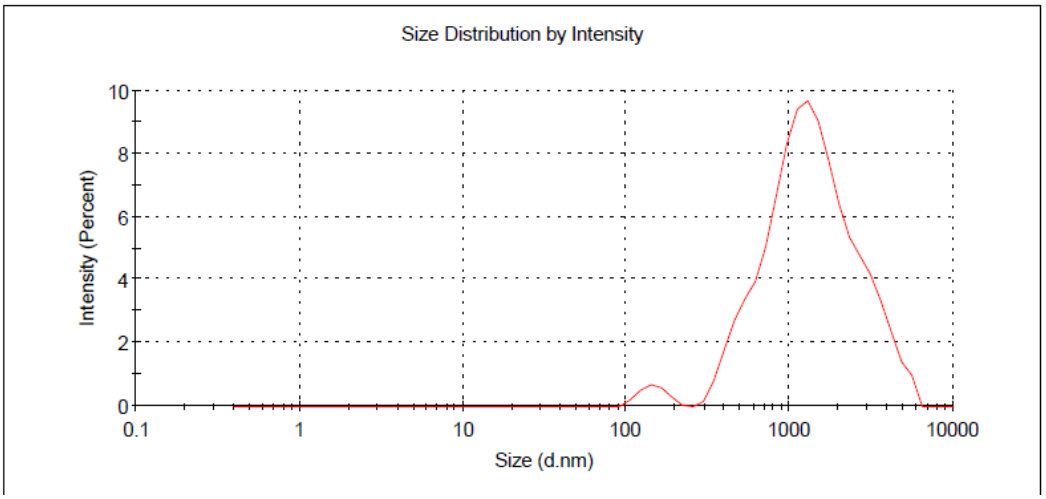

II. D_{px}10 (10 µM)-ctDNA (20 µM) in buffer

Results

		Size (d.nm):	% Intensity:	St Dev (d.n...
Z-Average (d.nm): 271.5	Peak 1:	355.3	98.2	204.2
PdI: 0.340	Peak 2:	5045	1.8	624.0
Intercept: 0.938	Peak 3:	0.000	0.0	0.000
Result quality : Good				

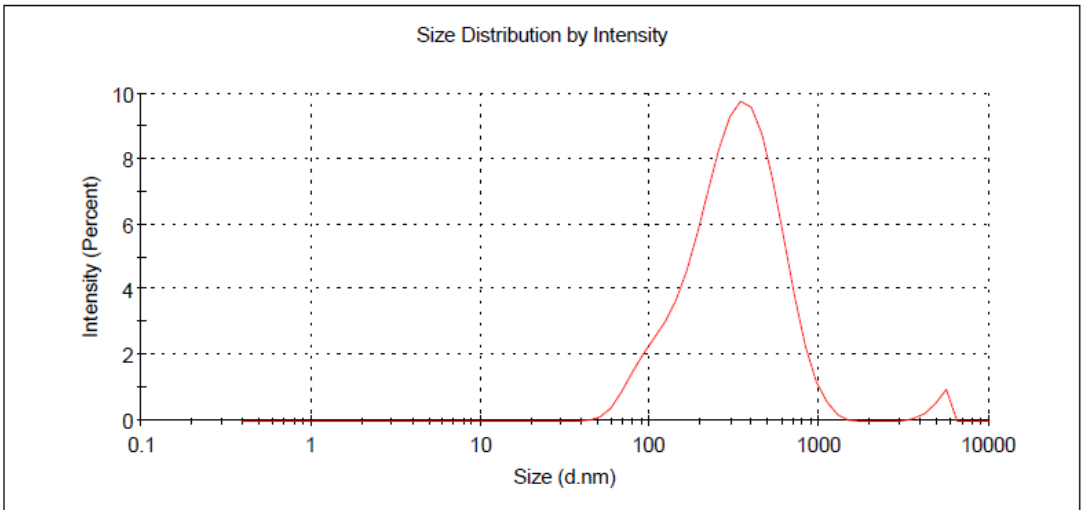

III. D_{px}12 (10 µM)-ctDNA (20 µM) in buffer

Results

		Size (d.nm):	% Intensity:	St Dev (d.n...
Z-Average (d.nm): 261.1	Peak 1:	387.9	100.0	296.5
PdI: 0.275	Peak 2:	0.000	0.0	0.000
Intercept: 0.935	Peak 3:	0.000	0.0	0.000
Result quality : Good				

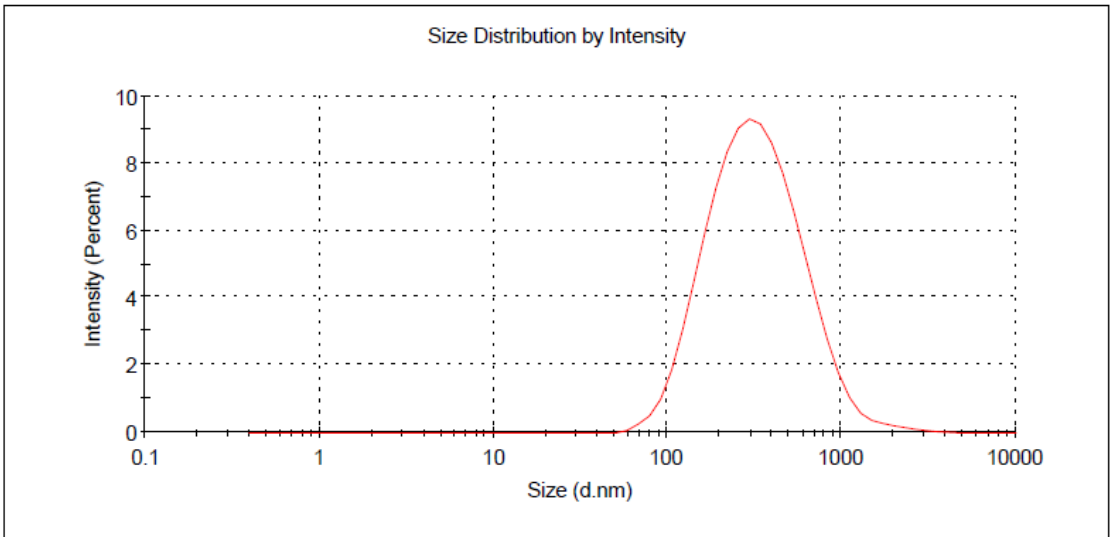

7. Zeta Potential Measurements

A. Zeta potential of only D_{px}Ns:

I. D_{px}6 (10 µM) in buffer

Results

			Mean (mV)	Area (%)	St Dev (mV)
Zeta Potential (mV):	22.3	Peak 1:	27.3	78.3	6.39
Zeta Deviation (mV):	9.59	Peak 2:	8.22	21.7	3.95
Conductivity (mS/cm):	0.366	Peak 3:	43.7	14.9	6.07

Result quality : See result quality report

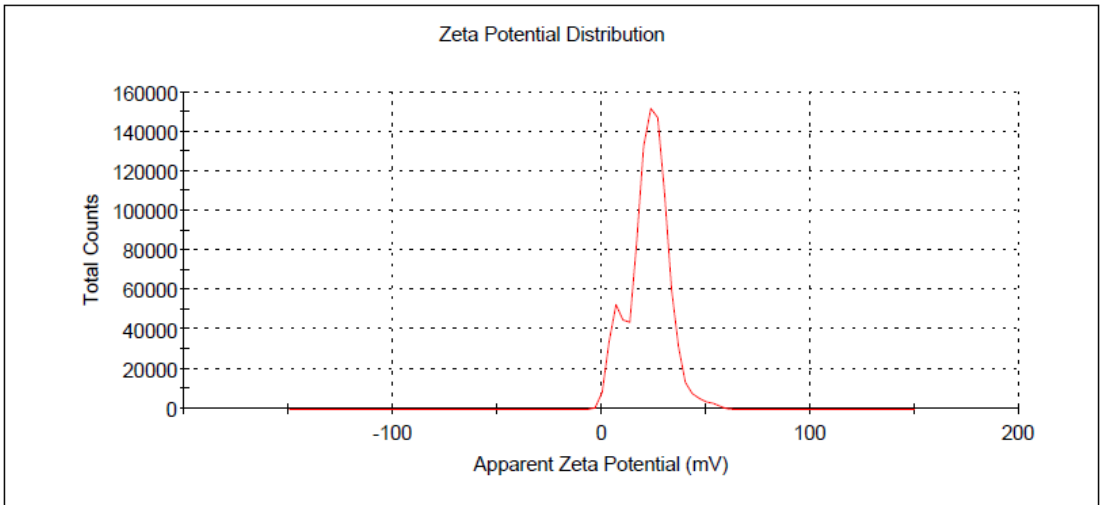

II. D_{px}10 (5 µM) in buffer

Results

			Mean (mV)	Area (%)	St Dev (mV)
Zeta Potential (mV):	23.8	Peak 1:	23.8	100.0	7.64
Zeta Deviation (mV):	7.36	Peak 2:	0.00	0.0	0.00
Conductivity (mS/cm):	0.224	Peak 3:	0.00	0.0	0.00

Result quality : Good

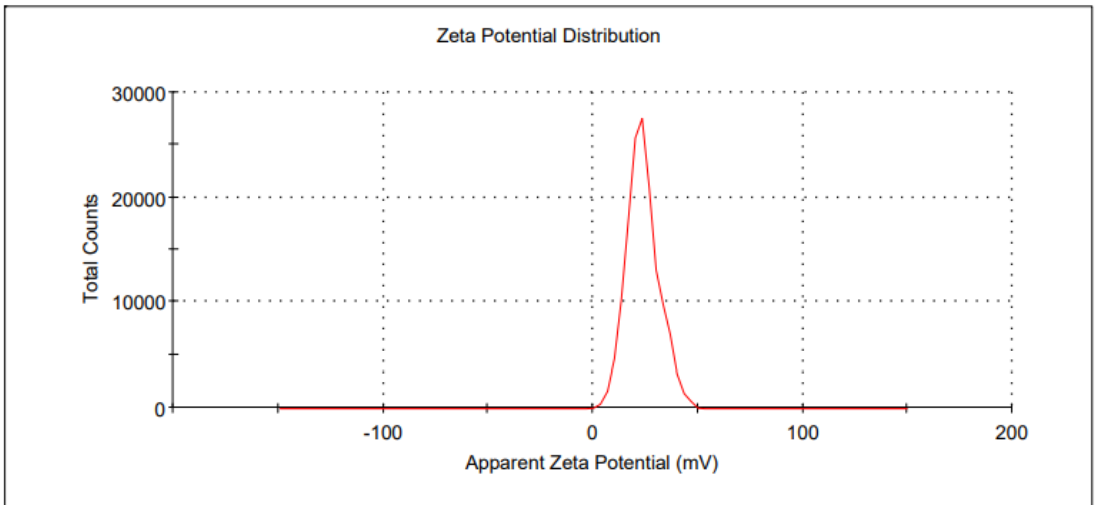

III. $D_{px}10$ (10 µM) in buffer

Results

		Mean (mV)	Area (%)	St Dev (mV)
Zeta Potential (mV): 31.6	**Peak 1:**	31.7	99.9	5.58
Zeta Deviation (mV): 5.56	**Peak 2:**	5.30	0.1	1.92
Conductivity (mS/cm): 0.366	**Peak 3:**	0.00	0.0	0.00
Result quality : Good				

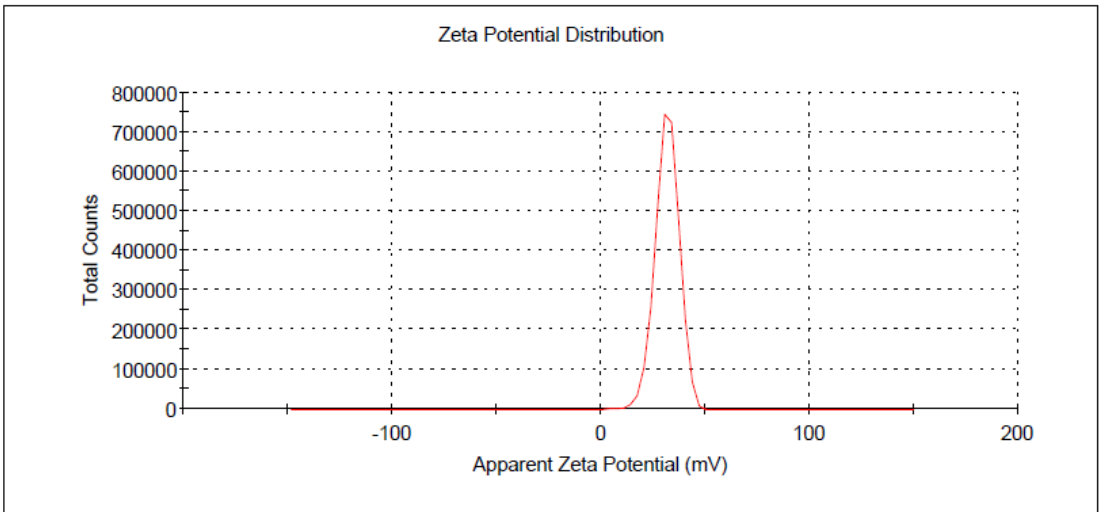

IV. $D_{px}12$ (5 µM) in buffer

Results

		Mean (mV)	Area (%)	St Dev (mV)
Zeta Potential (mV): 24.8	**Peak 1:**	24.9	100.0	6.18
Zeta Deviation (mV): 5.93	**Peak 2:**	41.4	1.2	1.64
Conductivity (mS/cm): 0.223	**Peak 3:**	0.00	0.0	0.00
Result quality : Good				

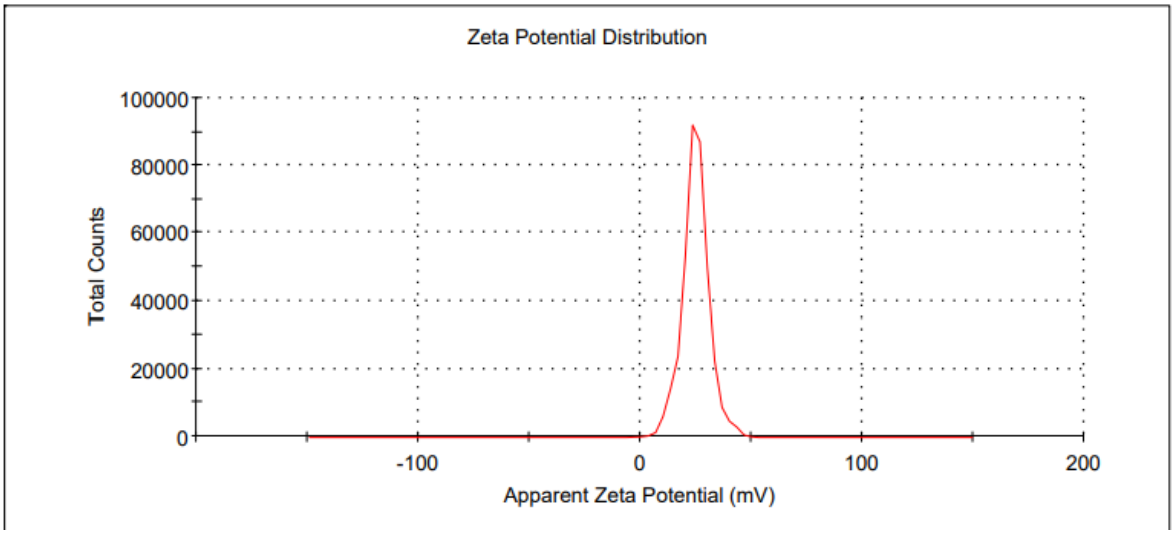

V. $D_{px}12$ (10 µM) in buffer

Results

		Mean (mV)	Area (%)	St Dev (mV)
Zeta Potential (mV): 27.8	Peak 1:	27.8	100.0	6.93
Zeta Deviation (mV): 6.79	Peak 2:	0.00	0.0	0.00
Conductivity (mS/cm): 0.366	Peak 3:	0.00	0.0	0.00
Result quality : Good				

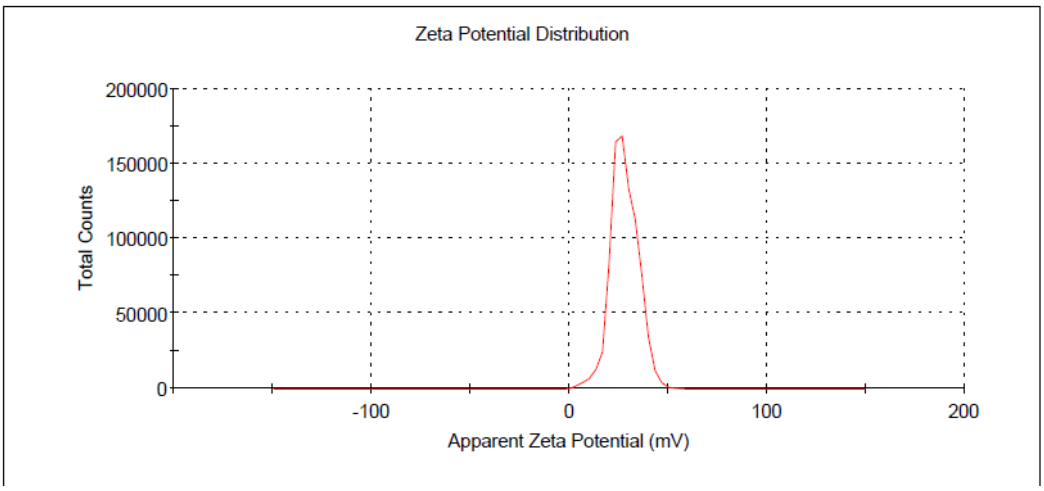

B. Zeta potential of D_{px}N-heparin co-assemblies:

I. $D_{px}6$ (5 µM)-heparin (10 µM) in buffer

Results

		Mean (mV)	Area (%)	St Dev (mV)
Zeta Potential (mV): -22.9	Peak 1:	-26.8	98.1	5.16
Zeta Deviation (mV): 9.07	Peak 2:	2.25	1.8	2.51
Conductivity (mS/cm): 0.215	Peak 3:	43.7	0.1	1.94
Result quality : Good				

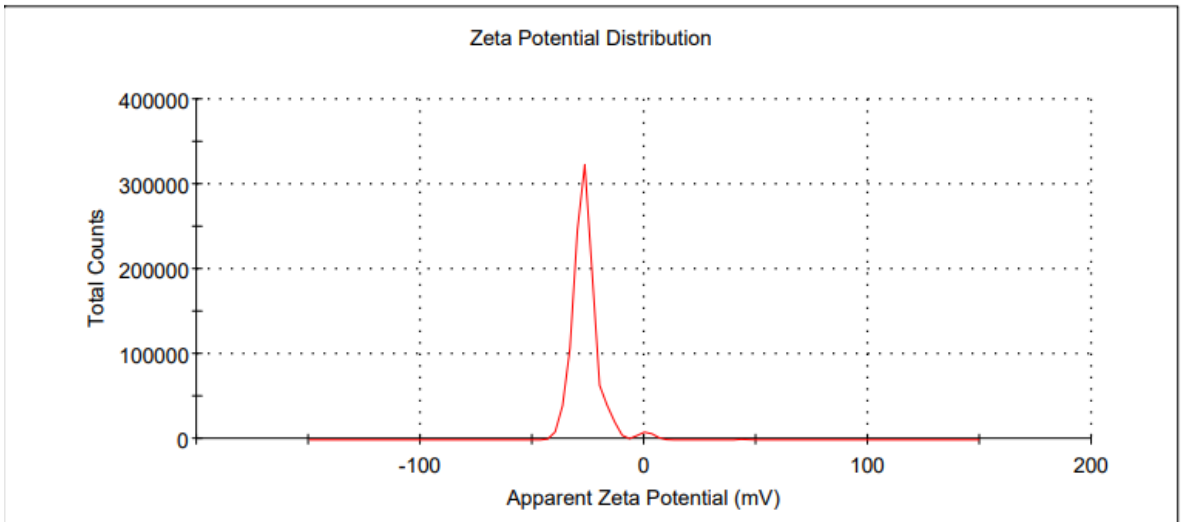

II. $D_{px}10$ (5 µM)-heparin (10 µM) in buffer

Results

			Mean (mV)	Area (%)	St Dev (mV)
Zeta Potential (mV):	-23.1	**Peak 1:**	-23.1	100.0	8.36
Zeta Deviation (mV):	8.32	**Peak 2:**	-7.72	11.5	3.18
Conductivity (mS/cm):	0.225	**Peak 3:**	0.00	0.0	0.00
Result quality :	Good				

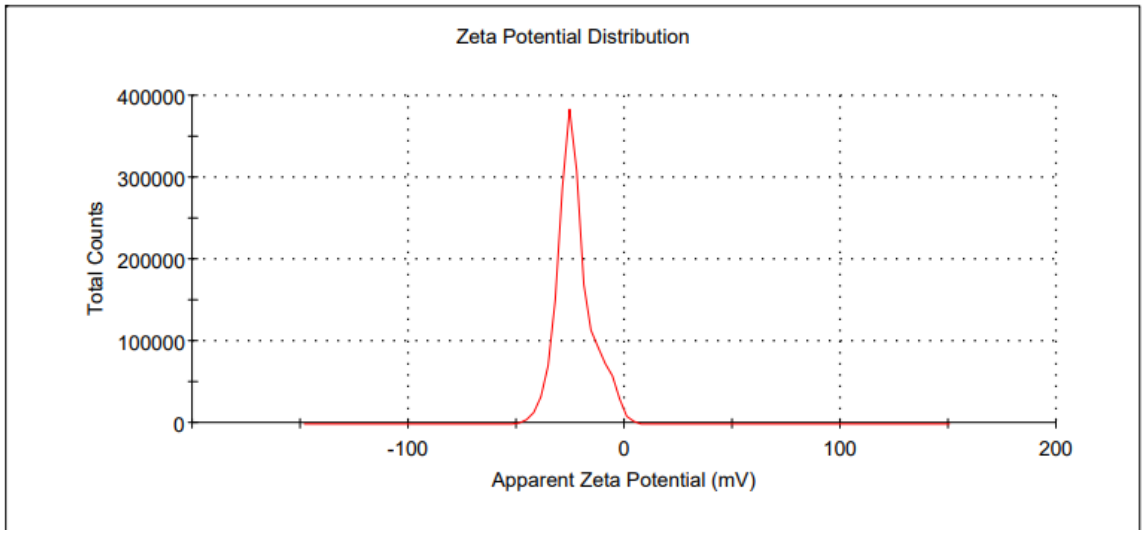

III. $D_{px}12$ (5 µM)-heparin (10 µM) in buffer

Results

			Mean (mV)	Area (%)	St Dev (mV)
Zeta Potential (mV):	-23.5	**Peak 1:**	-24.2	99.7	6.44
Zeta Deviation (mV):	8.68	**Peak 2:**	80.3	0.3	1.53
Conductivity (mS/cm):	0.231	**Peak 3:**	0.00	0.0	0.00
Result quality :	See result quality report				

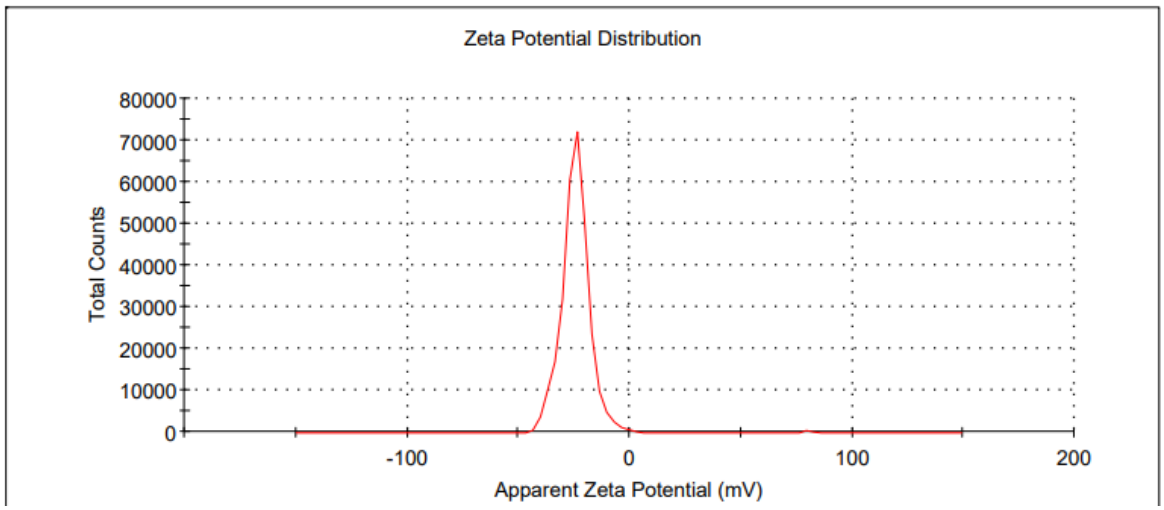

C. Zeta potential of D_{px}N-ctDNA co-assemblies:

I. D_{px}6 (10 µM)-ctDNA (20 µM) in buffer

Results

		Mean (mV)	Area (%)	St Dev (mV)
Zeta Potential (mV): 8.45	**Peak 1:**	8.45	100.0	2.94
Zeta Deviation (mV): 2.84	**Peak 2:**	0.00	0.0	0.00
Conductivity (mS/cm): 0.374	**Peak 3:**	0.00	0.0	0.00
Result quality : Good				

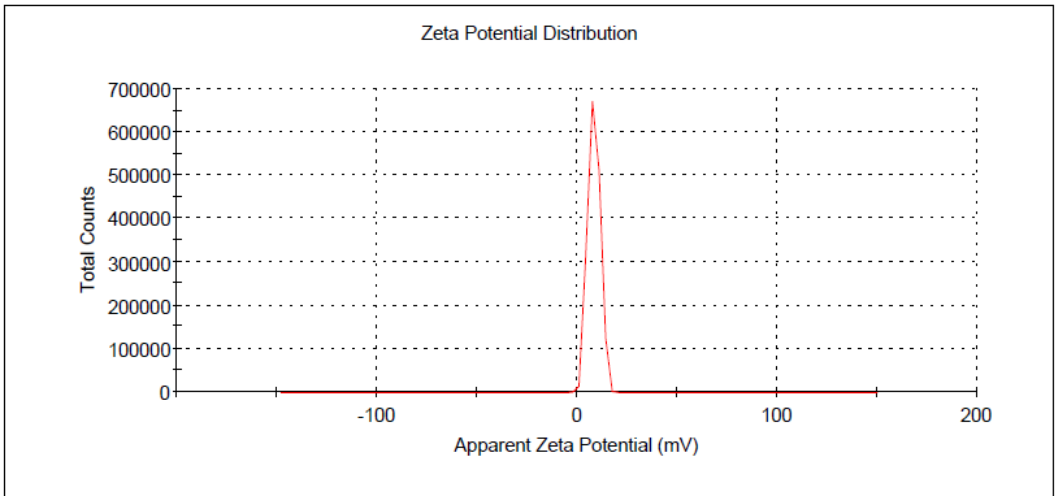

II. D_{px}10 (10 µM)-ctDNA (20 µM) in buffer

Results

		Mean (mV)	Area (%)	St Dev (mV)
Zeta Potential (mV): -36.9	**Peak 1:**	-36.8	100.0	5.34
Zeta Deviation (mV): 4.75	**Peak 2:**	0.00	0.0	0.00
Conductivity (mS/cm): 0.375	**Peak 3:**	0.00	0.0	0.00
Result quality : Good				

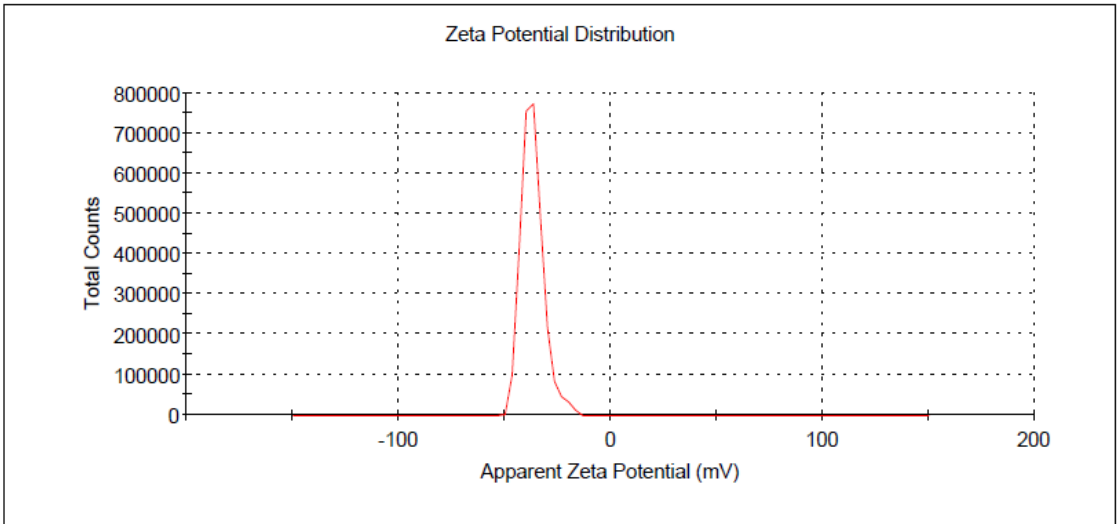

III. $D_{px}12$ (10 µM)-ctDNA (20 µM) in buffer

Results

		Mean (mV)	Area (%)	St Dev (mV)
Zeta Potential (mV):	-38.4	**Peak 1:** -38.4	100.0	5.34
Zeta Deviation (mV):	5.17	**Peak 2:** 0.00	0.0	0.00
Conductivity (mS/cm):	0.366	**Peak 3:** 0.00	0.0	0.00
Result quality :	Good			

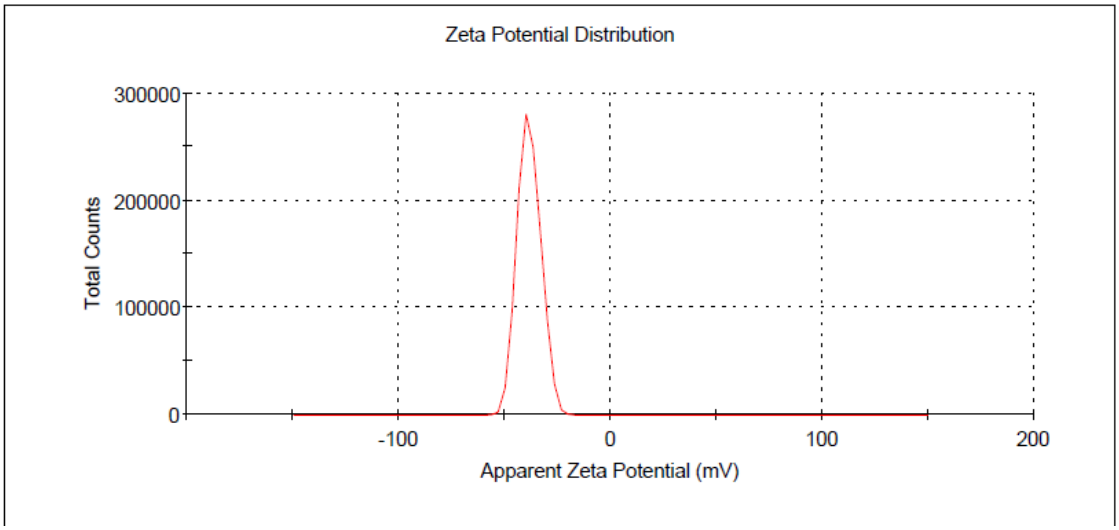

8. Time-Correlated Single Photon Counting (TCSPC) Measurements

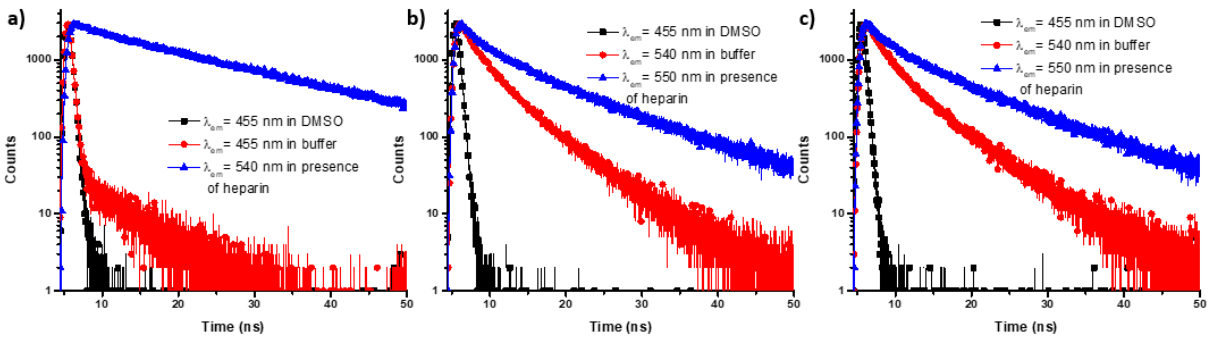

Fig. S38 Time-resolved decay profile of (a) **$D_{px}6$** (5 µM), (b) **$D_{px}10$** (5 µM) and (c) **$D_{px}12$** (5 µM) in DMSO, buffer and in presence of heparin (10 µM) in buffer. (λ_{ex} = 340 nm)

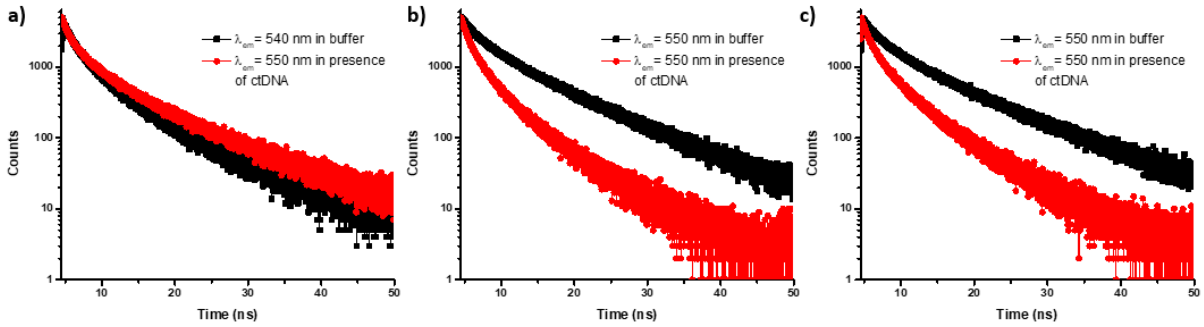

Fig. S39 Time-resolved decay profile of (a) **D*px*6** (10 µM), (b) **D*px*10** (10 µM) and (c) **D*px*12** (10 µM) without and with ctDNA (20 µM) in buffer. (λ_{ex} = 340 nm)

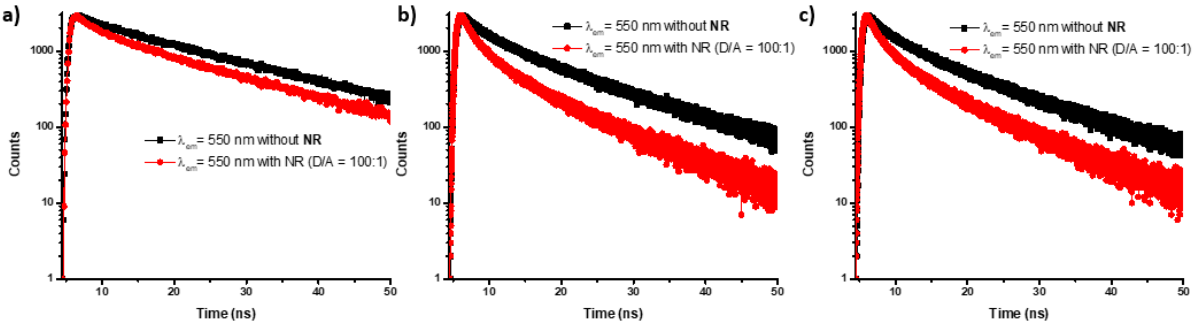

Fig. S40 Time-resolved decay profile of (a) **D*px*6** (5 µM)-heparin (10 µM), (b) **D*px*10** (10 µM)-heparin (10 µM) and (c) **D*px*12** (10 µM)-heparin (10 µM) without and with Nile Red (**NR**) (D/A = 100:1) in buffer. (λ_{ex} = 340 nm)

9. NMR Characterizations

A. ^{1}H NMR of C_6-CHO (500 MHz, $CDCl_3$):

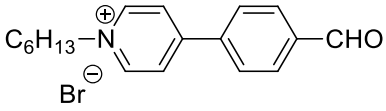

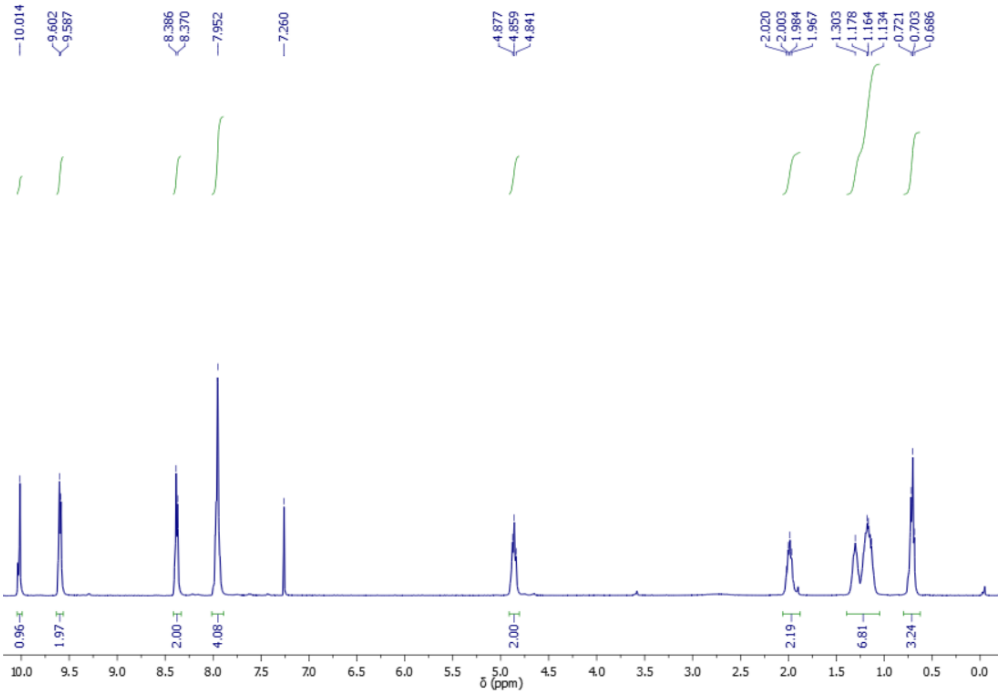

B. ^{13}C NMR of C_6-CHO (500 MHz, $CDCl_3$):

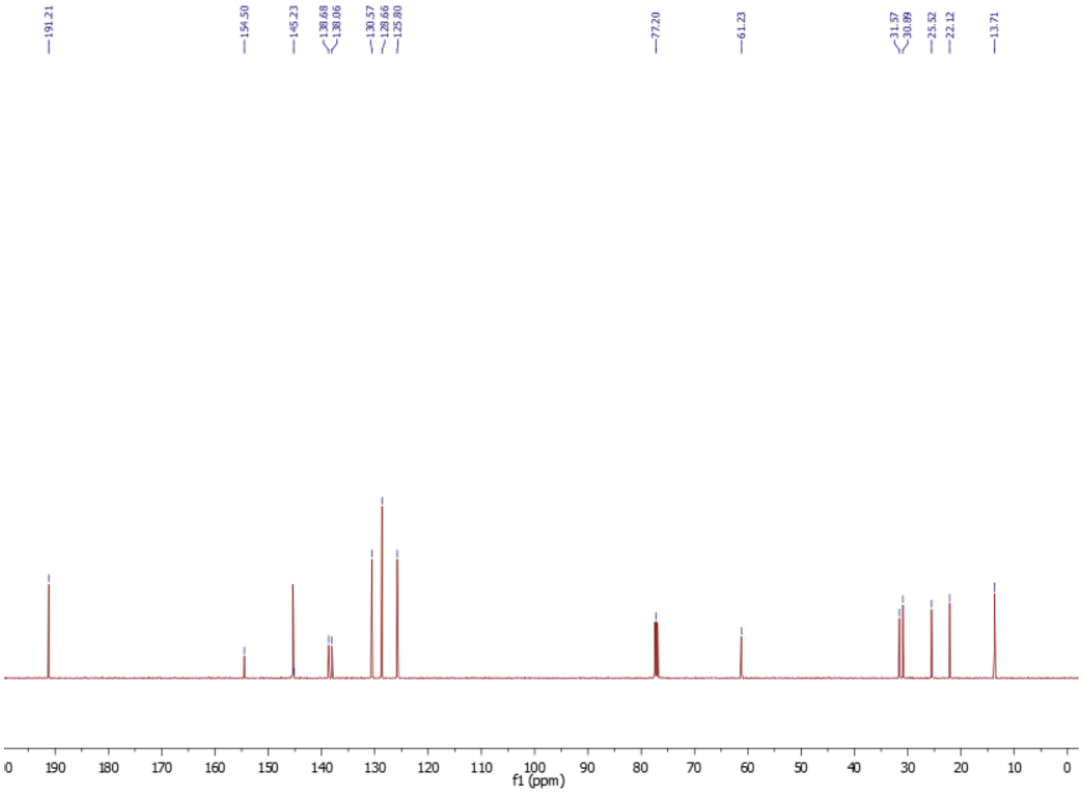

C. ^{1}H NMR of C_{10}-CHO (500 MHz, $CDCl_3$):

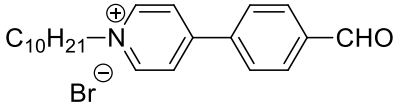

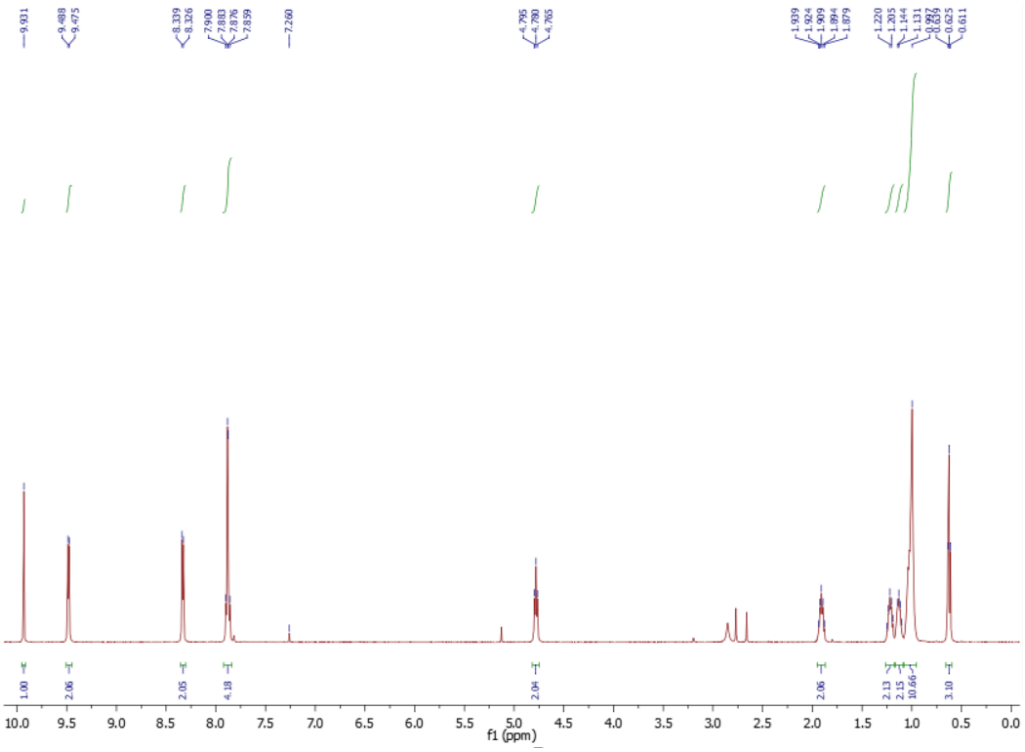

D. ^{13}C NMR of C_{10}-CHO (500 MHz, $CDCl_3$):

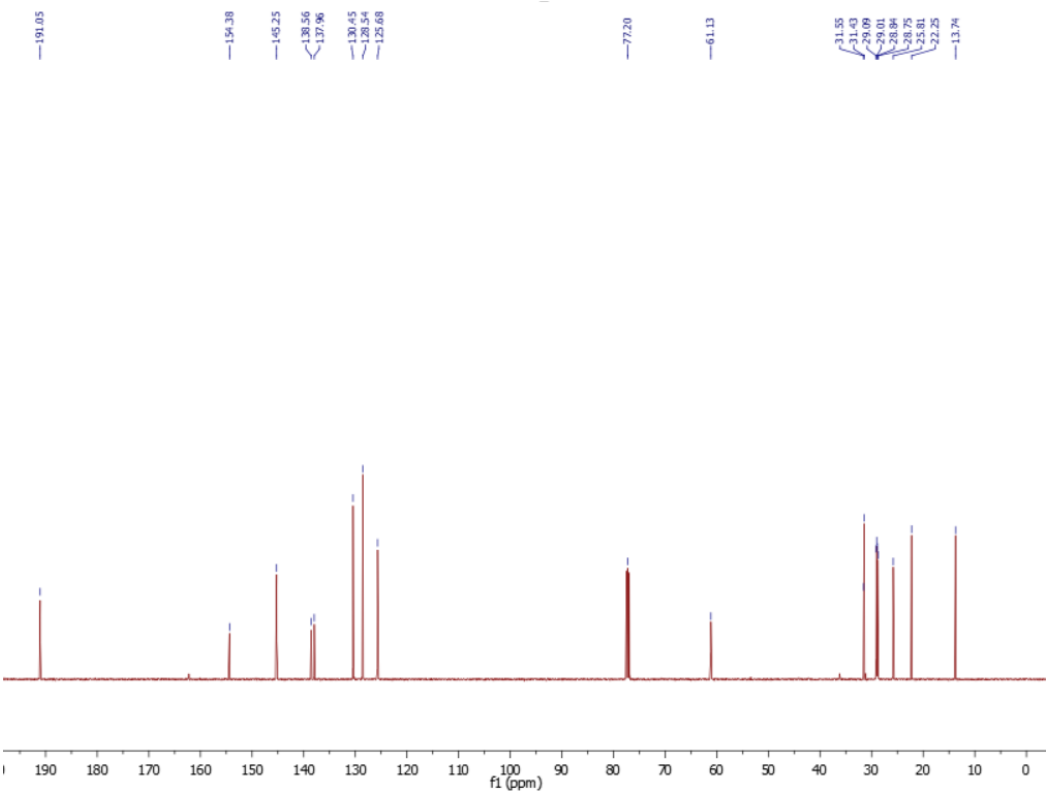

C. ^{1}H NMR of C_{12}-CHO (400 MHz, $CDCl_3$):

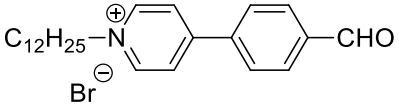

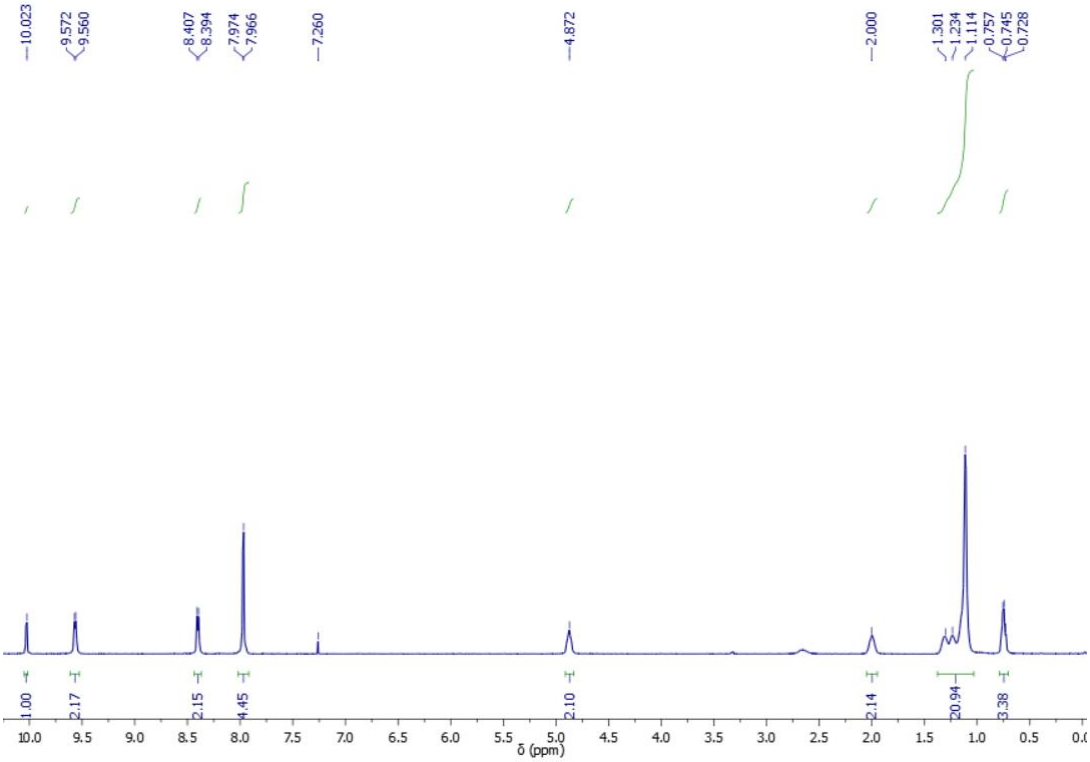

D. ^{13}C NMR of C_{12}-CHO (500 MHz, $CDCl_3$):

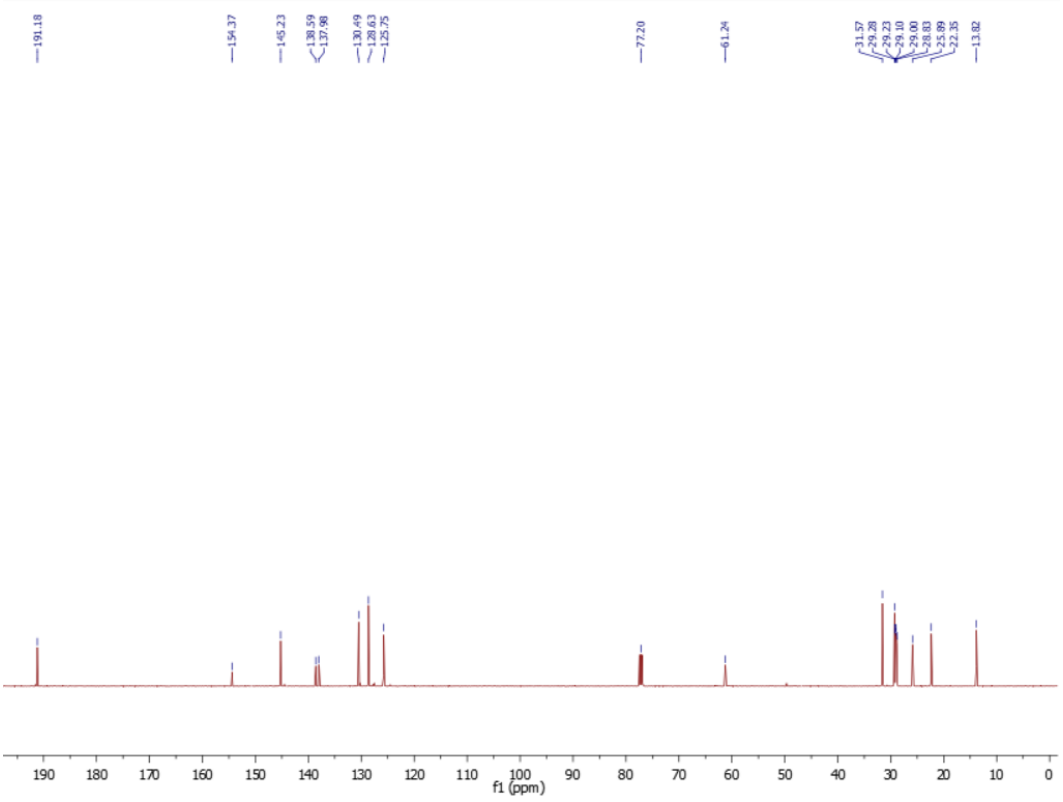

E. ^{1}H NMR of 6CS (500 MHz, DMSO-D$_6$):

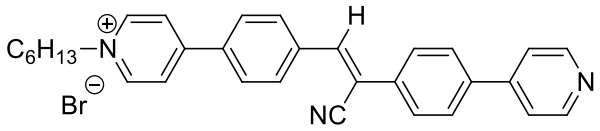

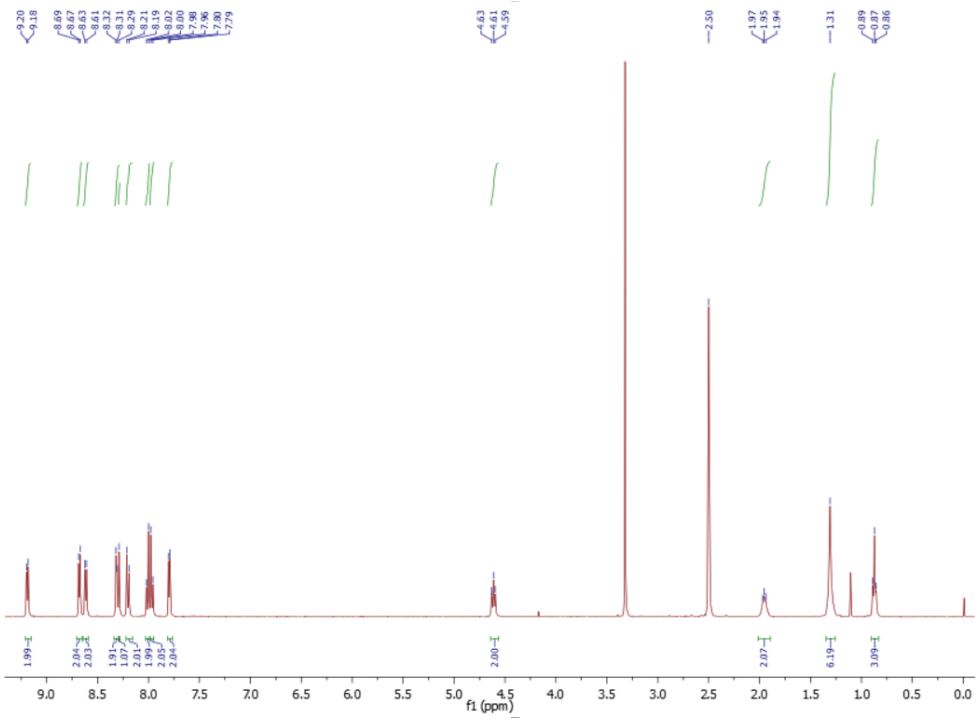

F. ^{13}C NMR of 6CS (400 MHz, DMSO-D$_6$):

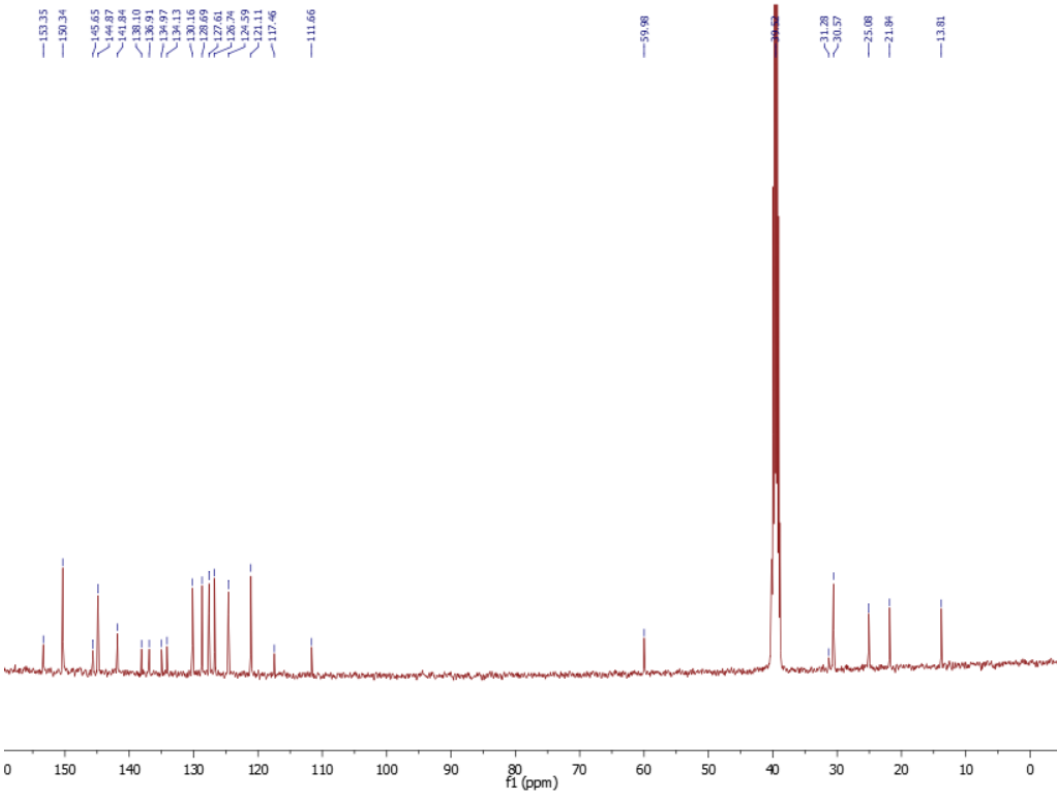

G. ^{1}H NMR of 10CS (500 MHz, DMSO-D$_6$):

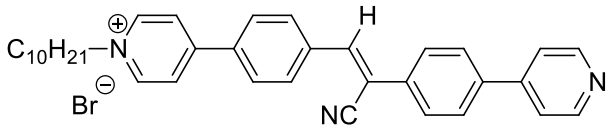

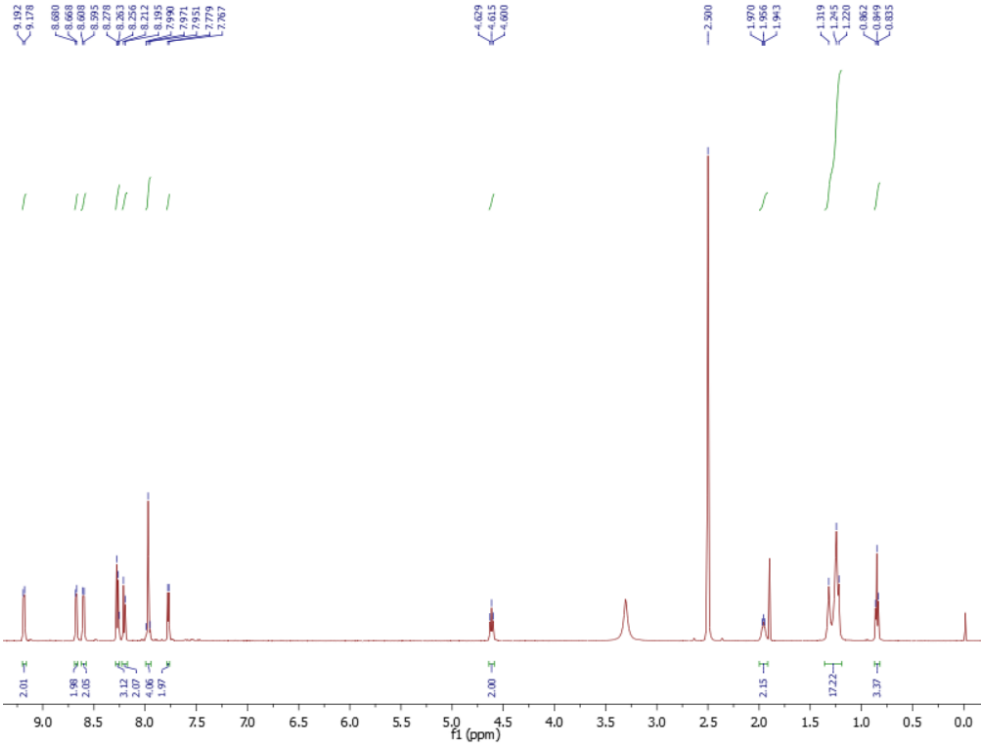

H. ^{13}C NMR of 10CS (500 MHz, DMSO-D$_6$):

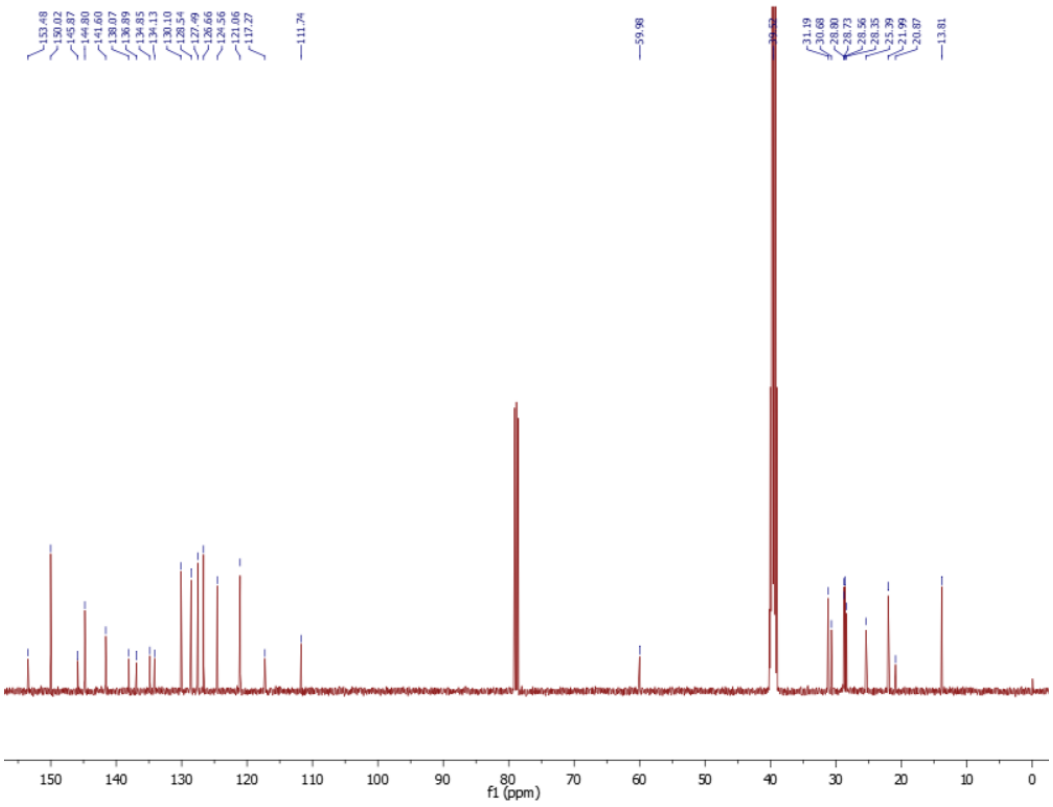

I. ^{1}H NMR of 12CS (400 MHz, DMSO-D$_6$):

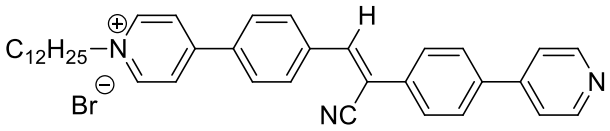

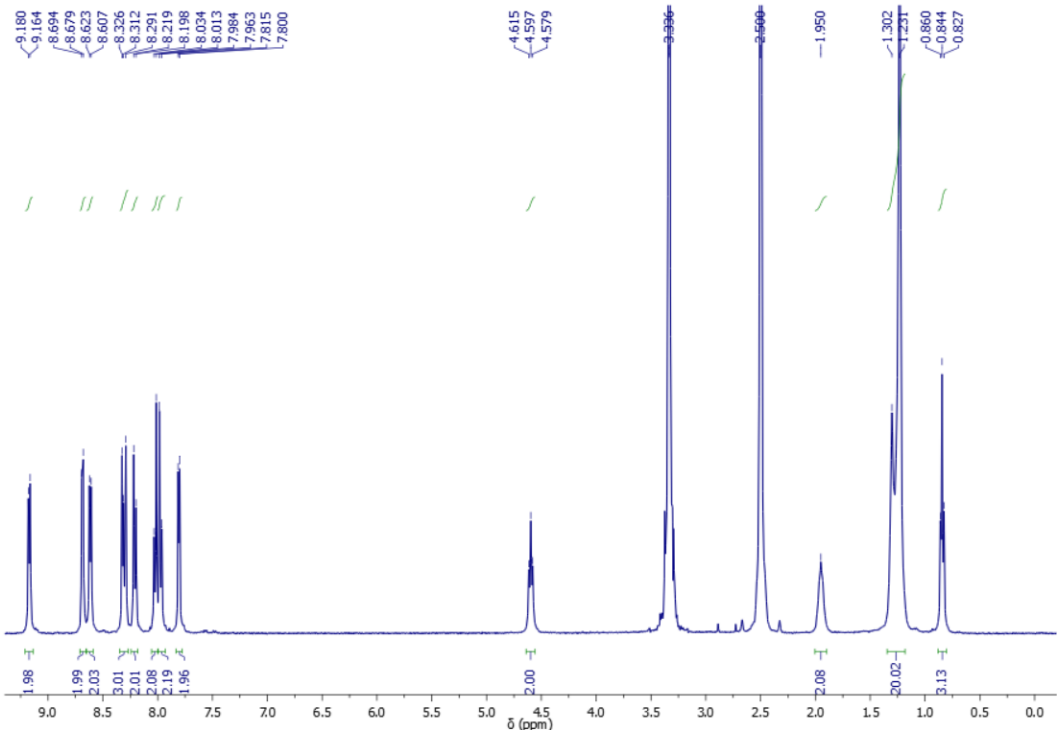

J. ^{13}C NMR of 12CS (500 MHz, DMSO-D$_6$):

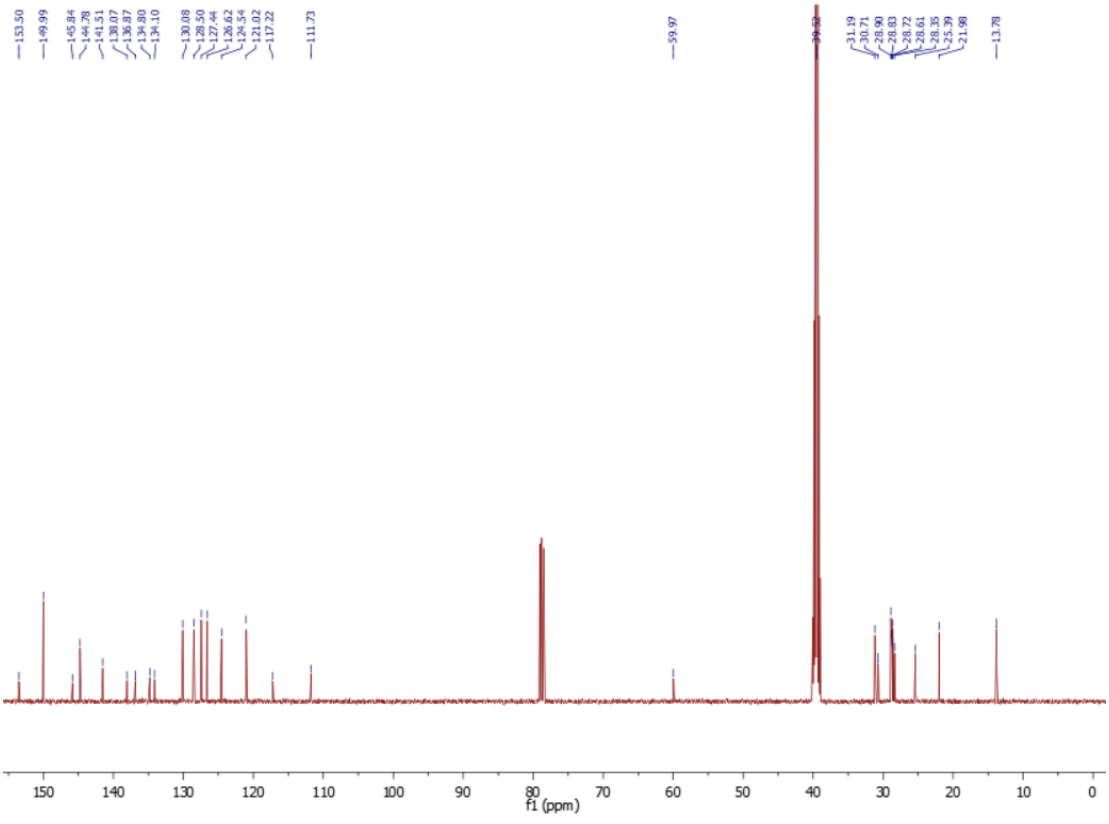

K. ^{1}H NMR of D$_{px}$6 (400 MHz, DMSO-D$_6$):

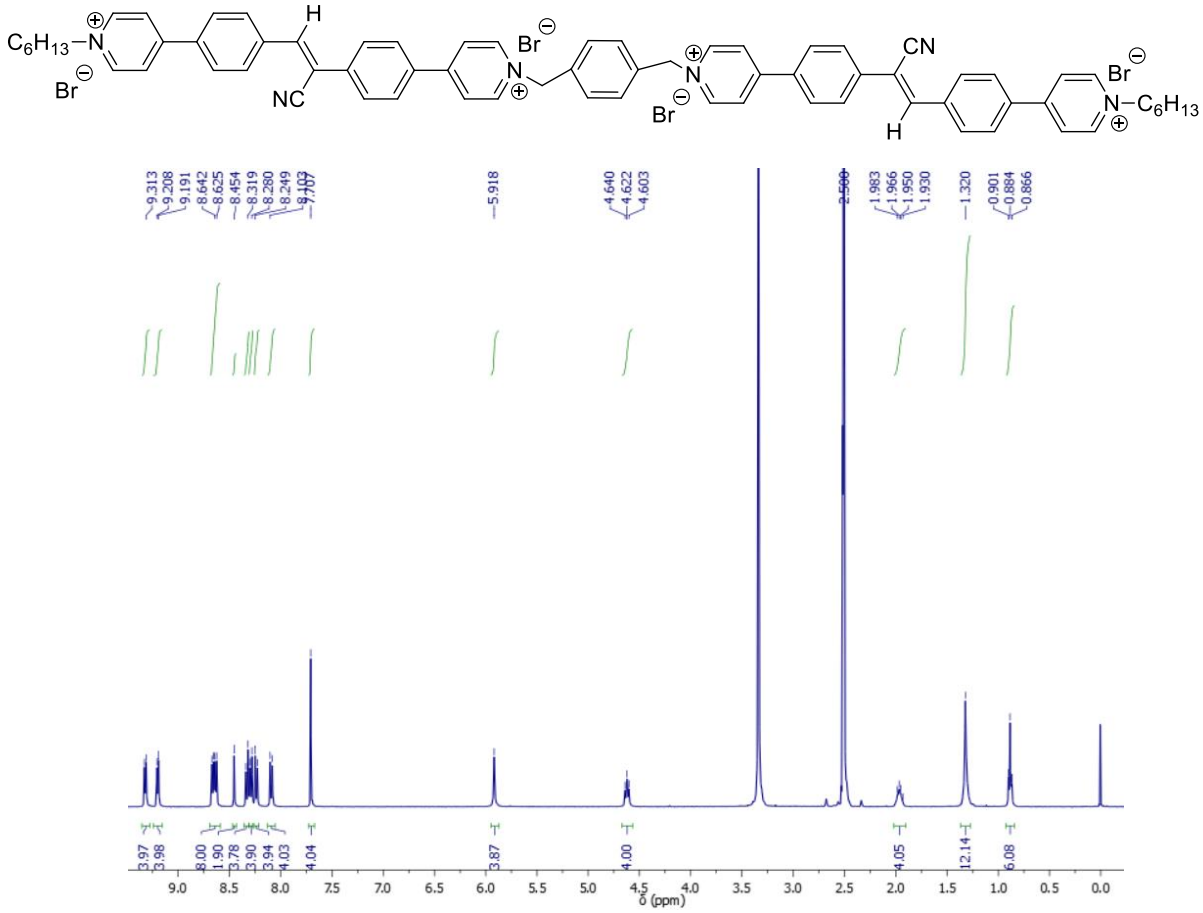

L. ^{13}C NMR of D$_{px}$6 (500 MHz, DMSO-D$_6$):

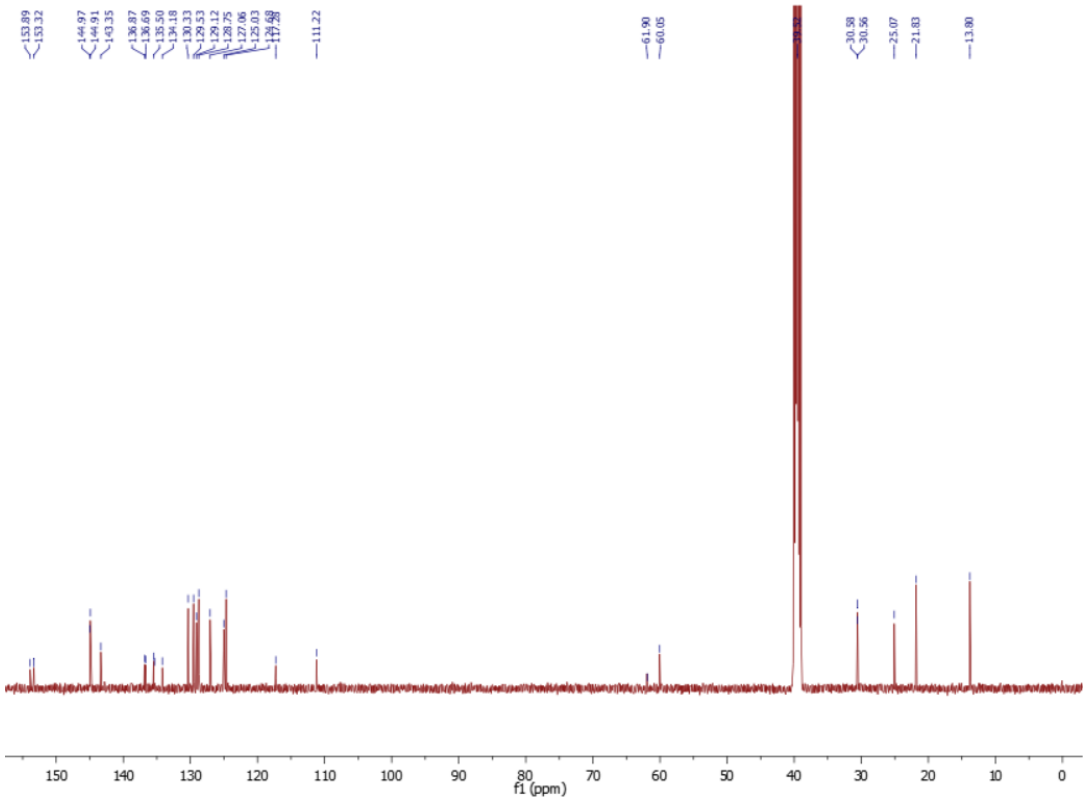

M. ^{1}H NMR of D$_{px}$10 (400 MHz, DMSO-D$_6$):

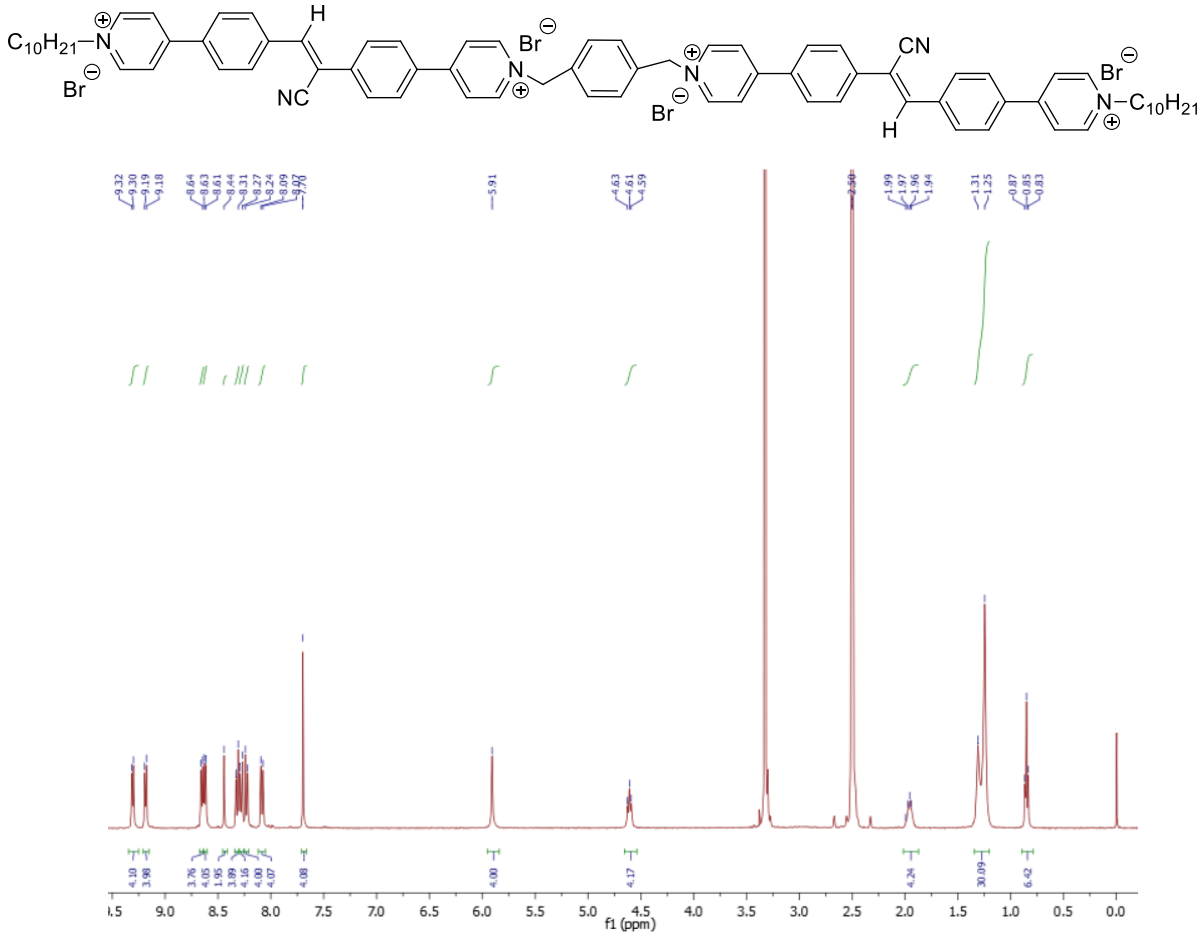

N. ^{13}C NMR of D$_{px}$10 (500 MHz, DMSO-D$_6$):

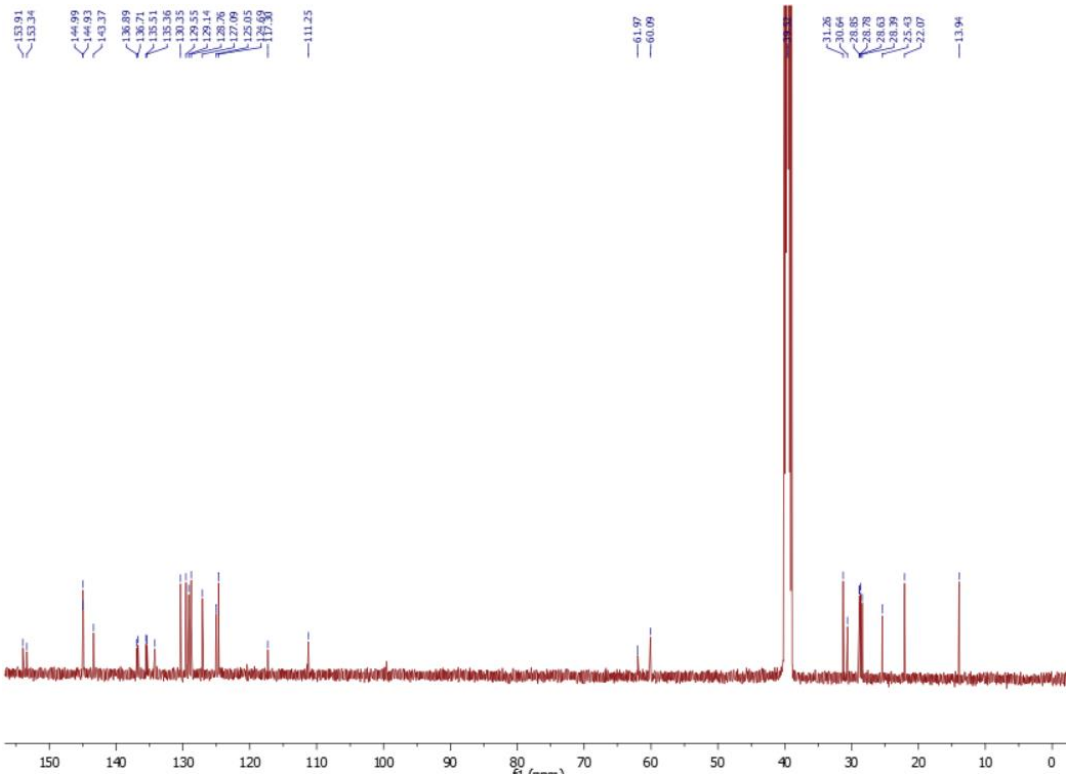

O. ^{1}H NMR of D$_{px}$12 (400 MHz, DMSO-D$_6$):

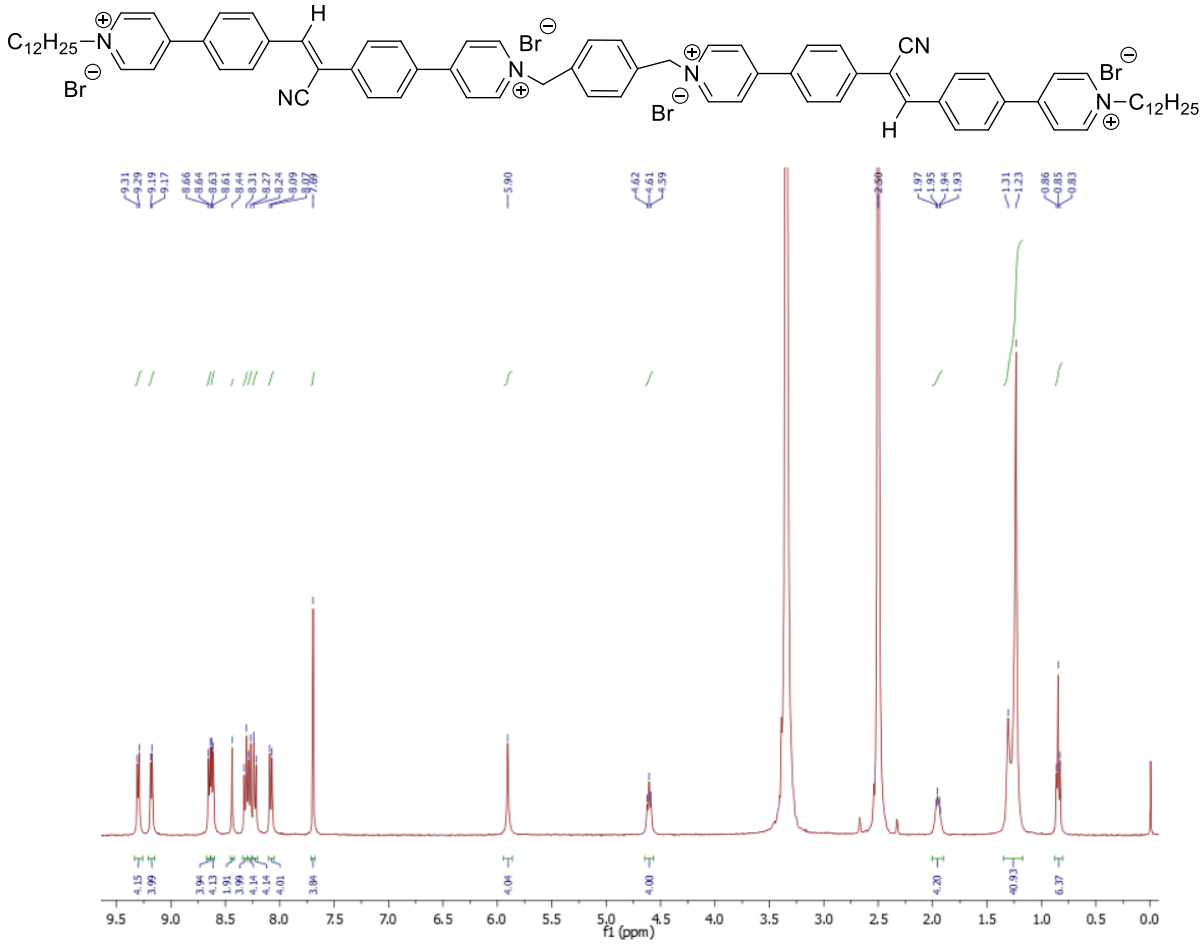

P. ^{13}C NMR of D$_{px}$12 (500 MHz, DMSO-D$_6$):